

General Disclaimer

One or more of the Following Statements may affect this Document

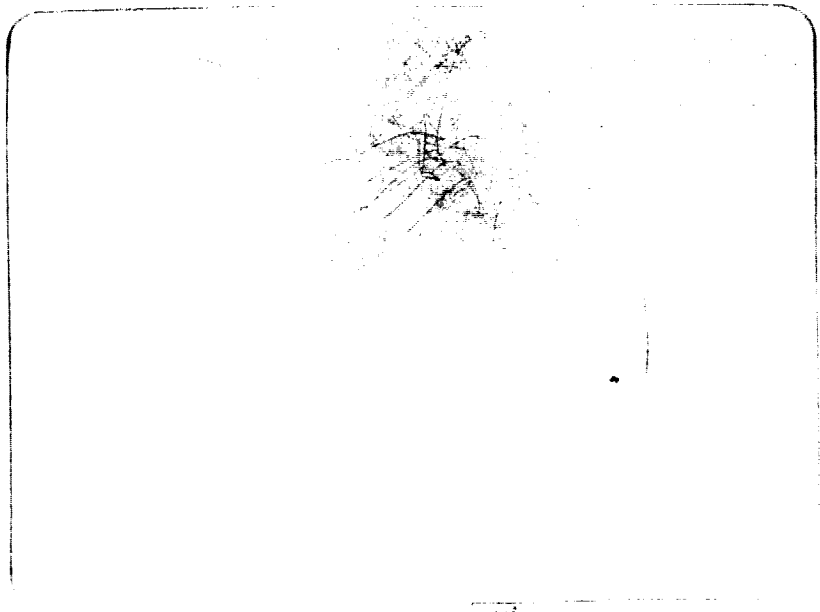
- This document has been reproduced from the best copy furnished by the organizational source. It is being released in the interest of making available as much information as possible.
- This document may contain data, which exceeds the sheet parameters. It was furnished in this condition by the organizational source and is the best copy available.
- This document may contain tone-on-tone or color graphs, charts and/or pictures, which have been reproduced in black and white.
- This document is paginated as submitted by the original source.
- Portions of this document are not fully legible due to the historical nature of some of the material. However, it is the best reproduction available from the original submission.

E82-10369

CR-169316



SECRETARIA DE PLANEJAMENTO DA PRESIDÊNCIA DA REPÚBLICA
CONSELHO NACIONAL DE DESENVOLVIMENTO CIENTÍFICO E TECNOLÓGICO



"Made available under NASA sponsorship
in the interest of early and wide dis-
semination of Earth Resources Survey
Program information and without liability
for any use made thereon."



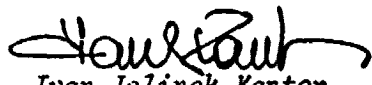
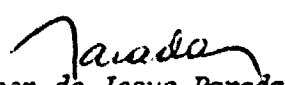
(E82-10369) COMPARISON OF STORM-TIME
CHANGES OF GEOMAGNETIC FIELD AT GROUND AND
AT MAGSAT ALTITUDES, PART 3 (Instituto de
Pesquisas Espaciais, Sao Jose) 54 p
HC A04/MF A01

N82-32791

Unclas
CSCL 04A G3/43 0369



INSTITUTO DE PESQUISAS ESPACIAIS

1. Publication N ^o INPE-2523-RPE/415	2. Version	3. Date Sept., 1982	5. Distribution <input type="checkbox"/> Internal <input checked="" type="checkbox"/> External <input type="checkbox"/> Restricted
4. Origin DGA/DIG	Program MATE		
6. Key words - selected by the author(s) GEOMAGNETIC VARIATIONS STORM-TIME CHANGES			
7. U.D.C.: 550.38			
8. Title COMPARISON OF STORM-TIME CHANGES OF GEOMAGNETIC FIELD AT GROUND AND AT MAGSAT ALTITUDES. PART III		INPE-2523-RPE/415	10. N ^o of pages: 54
			11. Last page: 52
9. Authorship Rajaram Purushottam Kane ✓ Nalin Babulal Trivedi			12. Revised by  Ivan Jelinek Kantor
Responsible author <i>Rajaram P. Kane</i>			13. Authorized by  Nelson de Jesus Parada Director
14. Abstract/Notes <p>The latitudinal distributions of ΔH, ΔX, ΔY, ΔZ were studied for quiet and disturbed periods. For quiet periods, the average patterns showed some variations common to Dusk and Dawn, thus indicating probable ground anomaly. However, there were significant differences too between Dusk and Dawn, indicating considerable diurnal variation effects. Particularly in ΔY, these effects were large and were symmetric about the dip equator. For disturbed day passes, the quiet day patterns were considered as base levels and the latter were subtracted from the former. The resulting residual latitudinal patterns were, on the average, symmetric about the geographical equator. However, individual passes showed considerable north-south asymmetries, probably indicating meanderings of the central plane of the magnetospheric ring current.</p>			
15. Remarks		<p style="text-align: center;">RECEIVED SEP 10, 1982 SIS/9026</p> <p>M-055 TYPE II</p>	

3rd MAGSAT Progress Report for Project M55 - August 1982

COMPARISON OF STORM-TIME CHANGES OF GEOMAGNETIC FIELD
AT GROUND AND AT MAGSAT ALTITUDES
PART III

Rajaram Purushottam Kane and Nalin Babulal Trivedi

Instituto de Pesquisas Espaciais - INPE
Conselho Nacional de Desenvolvimento Científico e Tecnológico - CNPq
12200 - São José dos Campos, SP, Brazil

Abstract

The latitudinal distributions of ΔH , ΔX , ΔY , ΔZ were studied for quiet and disturbed periods. For quiet periods, the average patterns showed some variations common to Dusk and Dawn, thus indicating probable ground anomaly. However, there were significant differences too between Dusk and Dawn, indicating considerable diurnal variation effects. Particularly in ΔY , these effects were large and were symmetric about the dip equator. For disturbed day passes, the quiet day patterns were considered as base levels and the latter were subtracted from the former. The resulting residual latitudinal patterns were, on the average, symmetric about the geographical equator. However, individual passes showed considerable north-south asymmetries, probably indicating meanderings of the central plane of the magnetospheric ring current.

3rd MAGSAT Progress Report for Project M55 - August 1982

COMPARISON OF STORM-TIME CHANGES OF GEOMAGNETIC FIELD
AT GROUND AND AT MAGSAT ALTITUDES
PART III

Rajaram Purushottam Kane and Nalin Babulal Trivedi

Instituto de Pesquisas Espaciais - INPE
Conselho Nacional de Desenvolvimento Científico e Tecnológico - CNPq
12200 - São José dos Campos, SP, Brazil

1. Introduction

The present investigation deals with the study of the storm-time variation at MAGSAT altitudes.

2. Techniques

From the data supplied to us on magnetic tape, the X, Y, Z components of the geomagnetic field were available for several passes. From these, the H component was obtained as $H = (X^2 + Y^2)^{1/2}$ and was expressed as $\Delta H = H$ (Observed) minus H (model). Similarly, ΔX , ΔY , ΔZ were obtained. The MAGSAT altitude at which these values are valid is not always constant and changes in the geocentric radius range $R = 6800 \pm 100$ km. Hence, these values were normalized to a constant geocentric distance $R_0 = 6800$ km by using an inverse R^3 relationship. This effect was only of the order of a few percent.

3. Accomplishments

In the NASA Technical Memorandum 82160 entitled "MAGSAT DATA PROCESSING: A REPORT FOR INVESTIGATORS" by R. Langel, J. Berbert, T. Jennings and R. Horner (Nov. 1981), the authors have reported values of ΔB at satellite for dip equator and D-EQL (Sugiura), relative equatorial disturbance in horizontal component for ground observatories. It would be interesting to see how our parameter ΔH compares with these.

Figure 1 shows a plot of ΔH_0 i.e. ΔH at geographic equator for Dusk (full lines) and Dawn (crosses) passes separately for the period Nov. 11-15, 1979. The top curve is for ΔH_0 (original). The second plot is for ΔH_0 (corrected) which is obtained by subtracting from ΔH_0 (original) the base-levels of ΔH_0 (i.e. average ΔH_0 for quiet periods) as described and given in the previous reports. Thus, ΔH_0 (corrected) for quiet period (e.g. Nov. 11-12) is almost zero, for Dawn as well as Dusk.

The third plot in Figure 1 is for ΔB and the fourth plot is for D-EQL (Sugiura). In general, all the four plots look similar. Two values of ΔB (marked as big dots) seem to be erroneous. Table 1 lists some erroneous values.

Figure 2 (left half) shows a plot of ΔH_0 (original) versus ΔB for Dusk and Dawn separately (upper and lower half). If some odd points (big dots) are ignored, excellent correlations are obtained with zero levels matching. Figure 2 (right half) shows ΔH_0 (corrected) versus ΔB . Here too, correlations are excellent; but the zero levels are different. Thus, ΔB matches almost completely with ΔH_0 (original). This is as expected.

Figure 3 (left half) shows ΔH_0 (original) versus D-EQL for Dusk passes. Correlation is high (+ 0.94) but some scatter is noticed. Figure 3 (right half) shows ΔH_0 (corrected) versus D-EQL.

Correlation is roughly the same. Thus, for Dusk passes, both ΔH_0 (original) and ΔH_0 (corrected) show good parallelism within a scatter of ± 10 nT.

Figure 4 shows similar plots for the Dawn passes. Here, correlations are lower (+ 0.76) and the scatter is large. Thus, ΔH_0 at the satellite and D-EQL at ground show a very good correlation for Dusk passes but not so good a correlation for Dawn passes. This is rather surprising; because, in the previous reports we have shown that for about a dozen observatories at different longitudes and latitudes (within $\pm 30^\circ$ of equator), the variations at ground and at satellite were very well correlated (+ 0.90 or more) for both Dawn and Dusk passes. May be that D-EQL as obtained by Sugiura has some uncertainties. This needs scrutiny.

So far, we concentrated attention on the equatorial values only. We now study the effects at other latitudes. Amongst the various passes (about 1200) for the period Nov. 2, 1979 - Jan. 18, 1980, there are a few during magnetically disturbed periods. Figure 5 shows the latitudinal variation of ΔH for the Dusk pass No. 184 which occurred at an equatorial longitude of about -79° i.e. $79^\circ W$. The original values are represented by the third plot (Figure 5(a), thin full line) and show a minimum at about -15° latitude. However, before concluding that the minimum is really at about -15° , it is necessary to check whether there is any permanent ground magnetic anomaly effect in this region. For this, the average latitudinal variation of six quiet-day (Dst within ± 10) Dusk passes which occurred in the longitude belt $75^\circ-80^\circ W$ was evaluated. The top curve (crosses) in Figure 5(b) shows the average pattern. As can be seen, the minimum at about -15° latitude is an inherent feature for this longitude belt, probably due to ground anomaly. For a correct estimate of the storm-time effect for pass 184, the top curve (average) should be subtracted from the third curve. The resulting corrected storm-time effect is shown by the second curve (Figure 5(c), full thick line) which shows a rather flat latitude distribution of storm-time ΔH for this pass.

To study the latitude distribution of storm-time effect for other passes, it was necessary to establish first the base levels i.e. average quiet-day latitudinal patterns of ΔH , ΔX , ΔY and ΔZ . For this, all passes were first sorted out according to 5° longitude belts viz, $\pm(0$ to $5^\circ)$, $\pm(5^\circ$ to $10^\circ)$ $\pm(175^\circ$ to $180^\circ)$ and then, in each group, the latitudinal patterns of all the quiet-day passes (Dst within ± 10) were averaged. Figure 6(a), (b), (c), (d) show the average quiet day patterns for ΔH for Dusk (left half) and Dawn (Right half) for successive 5° longitude belts. In general, patterns for Dusk and Dawn are roughly similar, indicating that there are some inherent ground anomaly effects common to both. If so, an average of the two should be a better estimate of such anomalies. Figure 7(a), (b), (c), (d) (left half) show a plot of ΔH (Dusk + Dawn)/2. A considerable anomaly is noticed in several longitude belts, notably the Bangui anomaly (Figure 7c) at about $6^\circ N$ in the 10 - $20^\circ E$ longitudes.

In a similar way, the factor ΔH (Dusk-Dawn)/2 would eliminate such a ground anomaly and one would obtain a measure of the difference in diurnal variation effects at Dusk and Dawn. The right half of Figure 7 shows ΔH (Dusk-Dawn)/2 (full lines). Changes of the order of a few nT are noticed, though the patterns are different in different longitude belts. To check whether the minima have any relationship with the dip equator rather than geographical equator, vertical arrows indicate the position of the dip equator. In general, it seems that the minima do coincide with the dip equator. The crosses and dashed lines represent the X component. The H and X components show almost identical variations.

Figure 8(a), (b), (c), (d) show ΔY (Dusk) on the left half and ΔY (Dawn) on the right half. In general, ΔY (Dusk) shows much larger variations than ΔY (Dawn). In a recent paper, Maeda et al. (1982) have showed this effect from the Magsat data and have commented that the D variation (i.e. Y variation) appears everyday on the low-latitude dusk side and is antisymmetric about the dip equator. In Figure 8, the vertical arrows show the position of the dip equator in

the various longitude belts. It does seem that the Y component has a strong transition from one side of the arrow to the other. However, some ΔY (Dawn) plots do show some variations, indicating that some ground anomaly effect may be present even in the Y component, for some longitudes. If so, ΔY (Dusk + Dawn)/2 would be a rough estimate of the same, whereas ΔY (Dusk-Dawn)/2 would be a pure estimate of the diurnal variation effect.

Figure 9 shows ΔZ (Dusk) and ΔZ (Dawn), only for the longitude region -90° to 0° , in which the dip equator has large latitudinal excursions, from 13° S to 10° N. Here again, ΔZ (Dusk) shows larger fluctuations. However, ΔZ (Dawn) shows large trends.

Figure 10 shows ΔY (Dusk-Dawn)/2 in the left half and ΔZ (Dusk-Dawn)/2 in the right half, for the longitude belt -90° to 0° . The arrows indicate the position of the dip equator. For ΔY , a clear transition from one side of the arrow to the other is seen. For ΔZ , such an effect is not clear.

Figure 11 shows the average curves for all longitudes. The upper half is for geographical latitudes -30° to $+30^{\circ}$. In the first column, the H variations (full lines) are almost the same as the X variations (crosses) and both have small magnitudes. In the second column for ΔY also, the variations are small. In all columns, the top curve is for Dusk, the second curve for Dawn, the third for (Dusk + Dawn)/2 and the fourth for (Dusk - Dawn)/2. In the last column, the Z variations are also small except for some trends. Thus the geographical latitude distributions of the variations of H, X, Y, Z are all small.

The lower half of Figure 11 represents average distributions for dip latitudes. Here, the most conspicuous variation is that of ΔY (Dusk). In contrast, ΔY (Dawn) is negligibly small and hence both ΔY (Dusk + Dawn)/2 and ΔY (Dusk - Dawn)/2 are similar to

ΔY (Dusk) but roughly half in magnitude. Thus, amongst all these parameters, only ΔY (Dusk) has a significant dip-latitude dependence.

Maeda et al. (1982) have interpreted this dependence as indicative of meridional current systems in the equatorial ionosphere. However, we are not quite sure about the association of these currents with the equatorial electrojet, as envisaged in the Untiedt (1967) and Sugiura and Poros (1969) models. Because in that case, the electrojet itself should be strong. In the present case, the X component shows very little variations, showing that the main electrojet is not strong at dusk hours. Thus, strong meridional currents cannot exist at dusk because of the electrojet which is weak. To us, it seems that the presence of strong ΔY in the absence of strong ΔX indicates the usual Sq pattern of roughly circular currents, which, near midday, are mostly east-west but which, at dawn or dusk, are mostly north-south. In the equatorial region, longitudinal differences could then arise from the excursions of the Sq current system of one hemisphere into the other (Hutton 1967 a,b) and/or due to solstitial Sq currents through the magnetosphere (Van Sabben, 1970). Since the present investigation is not directly related to the quiet-time variations, we will not discuss or explore this matter any further but will only use these quiet-time patterns as base levels for subtracting from the disturbed-day patterns. The quiet-day pattern values for ΔH , ΔX , ΔZ for Dusk, Dawn, (Dusk + Dawn)/2 and (Dusk-Dawn)/2 are given in Tables 2,3 ... etc., as these may prove useful for other workers.

As shown in Figure 1, the period Nov. 11-15, 1979 was a storm period. On Nov. 13, pass 170 was only moderately disturbed (Dst = -17). However, the successive passes 171, 172 etc. were highly disturbed. In Figure 12, we show the latitude distributions of ΔH (full lines) and ΔX (crosses) for the Dusk passes 170-181 in the left half, continued for pass 182-188 in the upper right half. The vertical arrows indicate the position of the dip equator. All passes are corrected for base levels as illustrated in Figures 5.

It seems from Figure 12 that the ΔH or ΔX variations are not always symmetric about the geographical or dip equators. In the early passes, the Northern Hemisphere has larger storm effects. By about pass 178, the pattern is roughly symmetrical. For later passes, the Southern Hemisphere has larger storm effects. Thus, the storm-effects are not only not maximum either at the geographical or the dip equator but the nature of the north-south asymmetry changes during the course of the storm. In this case, the earlier part of the storm was stronger in the Northern Hemisphere. However, in the bottom of the right half of Figure 12, we show similar plots for the Dusk passes 936 to 939, which occurred during a disturbed period. Here, the storm-effect is larger in the Southern Hemisphere even in these initial passes of this storm of Jan.80. Thus, the conclusion would be that the north-south asymmetry could exist in any form at any stage of the storm.

In the middle of the right half of Figure 12, we show a similar plot for the disturbed day Dawn pass 184. In contrast to the Dusk pass 184, the Dawn pass shows very erratic latitudinal distribution, with no semblance of any maximum storm effect near either the geographic or the dip equator. Instead, one notices maximum storm effects at about $\pm 15^\circ$ geographical latitudes. For other Dawn passes on disturbed days, some other, different, patterns were noticed. Thus, the storm-time latitude distribution of ΔH or ΔX for Dawn passes seems to be erratic. We suspect that a considerable part of these erratic patterns as well as the north-south asymmetries may be related to latitudinal meandering of the central plane of the magnetospheric ring current and/or complications due to field-aligned currents, different in different local time zones.

Figure 13 shows similar plots for the Y component. Here, symmetry about the geographic or the dip equator seems to be more an exception than a rule. In general, the Y variation is erratic, with no systematic variation from one pass to the next, again probably indicating an erratic meandering of the central plane of the magnetospheric ring current during the course of the storm.

Figure 14 shows the latitudinal patterns of ΔX and ΔY averaged for all the storm-time passes 170-188. The upper half has geographical latitude as abscissa. ΔX shows a maximum storm effect (largest negative values) near the geographical equator (at about 5°S) with roughly a $\cos \theta$ dependence on either side. However, ΔY does not show any such effect clearly. Instead, one observes a minimum storm effect (smallest negative values) at about -10° i.e. 10° South latitude. Thus, on the average, the central plane of the storm-time ring current is almost coincident with the geographical equatorial plane, with a probable shift slightly southwards.

The lower half of Figure 14 shows similar average latitudinal patterns of ΔX and ΔY with dip latitude as abscissa. As can be seen, no clear latitude dependence is noticed, for either ΔX or ΔY . Thus, the storm-time ring current does not seem to be influenced by the dip equator.

4. Summary of the significant results

The average latitude dependence of the storm-time H or X variation is roughly symmetric about the geographic equator but not about the dip equator. Also, for individual passes, the pattern is generally not symmetric, the storm-effects being significantly larger in one hemisphere as compared to the other. For the Y component, no clear latitude dependence is noticed.

5. Future plans

The present investigation is now concluded.

References

- Hutton R. Sq currents in the American equatorial zone during the IGY-I. Seasonal effects. J. Atmos. Terr. Phys. 29, 1411-1427, 1967 (a)
- Hutton R. Sq currents in the American equatorial zone during the IGY-II Day to day variability. J. Atmos. Terr. Phys. 29, 1429, 1967(b)
- Maeda H., Iyemori T., Araki T and Kamei T. New evidence of meridional current system in the equatorial ionosphere. Geophys. Res. Letters 9, 337-340 (1982)
- Sugiura M. and Poros D.J. An improved model equatorial electrojet with a meridional current system. J. Geophys. Res. 74, 4025-4034 (1969)
- Untiedt J. A model of the equatorial electrojet involving meridional currents. J. Geophys. Res. 72, 5799-5810 (1967)
- Van Sabben D. Solstitial Sq - currents through the magnetosphere. J. Atmos. Terr. Phys. 32, 1331-1336 (1970)

Caption for Figures

Fig. 1 - Plot of ΔH_0 (i.e. ΔH at equatorial crossing, original as well as corrected for base level), ΔB (total field at dip equator) and D-EQL (Equatorial disturbance index for ground), for Nov. 11-15, 1979 for Dawn (full lines) and Dusk (crosses and dashes).

Fig. 2 - Upper half, ΔH_0 Dusk (original and corrected) versus ΔB Dusk (original). Lower half, ΔH_0 Dawn (original and corrected) versus ΔB Dawn (original).

Fig. 3 - ΔH_0 Dusk (original and corrected) versus D-EQL Dusk (by Sugiura, for ground stations). Regression lines for direct and reverse correlations are marked.

Fig. 4 - ΔH_0 Dawn (original and corrected) versus D-EQL Dawn (by Sugiura, for ground stations). Regression lines for direct and reverse correlations are marked.

Fig. 5 - Latitudinal variation of ΔH for
(a) The specific disturbed-day Dusk pass No. 184 at longitude -79° .
(b) Quiet day base level obtained as average for six quiet-day passes in the longitude belt 75° - 80° W.
(c) The difference (a) minus (b).

Fig. 6 - Average latitudinal patterns of ΔH (Dusk) (left half) and ΔH (Dawn) (right half) for successive 5° longitude belts for the longitude ranges (a) longitude -180° to -90° , (b) longitude -90° to 0° , (c) longitude 0° to $+90^\circ$ and (d) longitude $+90^\circ$ to $+180^\circ$, + = East, - = West.

Fig. 7 - Average latitudinal variations for ΔH (Dusk + Dawn)/2 (left half) and ΔH (Dusk-Dawn)/2 (right half, full lines) for successive 5° longitude intervals for the longitude ranges (a) longitude -180° to -90° , (b) longitude -90° to 0° , (c) longitude 0° to $+90^\circ$ and (d) longitude $+90^\circ$ to $+180^\circ$. In the right half, crosses and dashes represent the X component and vertical arrows indicate the position of the dip equator.

Fig. 8 - Average latitudinal variations for ΔY (Dusk) (left half) and ΔY (Dawn)(right half) for successive 5° longitude belts for the longitude ranges (a) longitude -180° to -90° , (b) longitude -90° to 0° , (c) longitude 0° to $+90^\circ$ and (d) longitude $+90^\circ$ to $+180^\circ$. Vertical arrows indicate the position of the dip equator.

Fig. 9 - Average latitudinal variations for ΔZ (Dusk) (left half) and ΔZ (Dawn) (right half) for 5° longitude belts in the longitude range -90° to 0° , in which the position of the dip equator (vertical arrows) changes rapidly.

Fig. 10 - Average latitudinal variations for ΔY (Dusk-Dawn)/2 (left half) and ΔZ (Dusk-Dawn)/2 (right half) for 5° longitude belts in the longitude range -90° to 0° . Vertical arrows indicate the position of the dip equator.

Fig. 11 - Average latitudinal variations for ΔH and ΔX (first column, full lines and crosses), ΔY (second column) and ΔZ (third column) for Dusk, Dawn, (Dusk + Dawn)/2, (Dusk-Dawn)/2. The upper half has abscissa as geographical latitude while the lower half has abscissa as dip latitude.

Fig. 12 - Latitudinal variation of ΔH (full lines) and ΔX (crosses and dashes) corrected for base levels, for the Dusk passes 170-188 during the storm of Nov. 11-15, 1979, as also for the Dawn pass 184 and for the Dusk passes 936-939 in Jan. 1980. The pass number, longitude and Dst are indicated for each pass. Vertical arrows indicate the position of the dip equator.

Fig. 13 - Same as Fig. 12, but for ΔY .

Fig. 14 - Average latitudinal distribution of ΔX and ΔY for the storm-time Dusk passes 170-188 on Nov. 13-14, 1979.
Upper half - For geographical latitudes.
Lower half - For dip latitudes.

ORIGINAL PAGE IS
OF POOR QUALITY

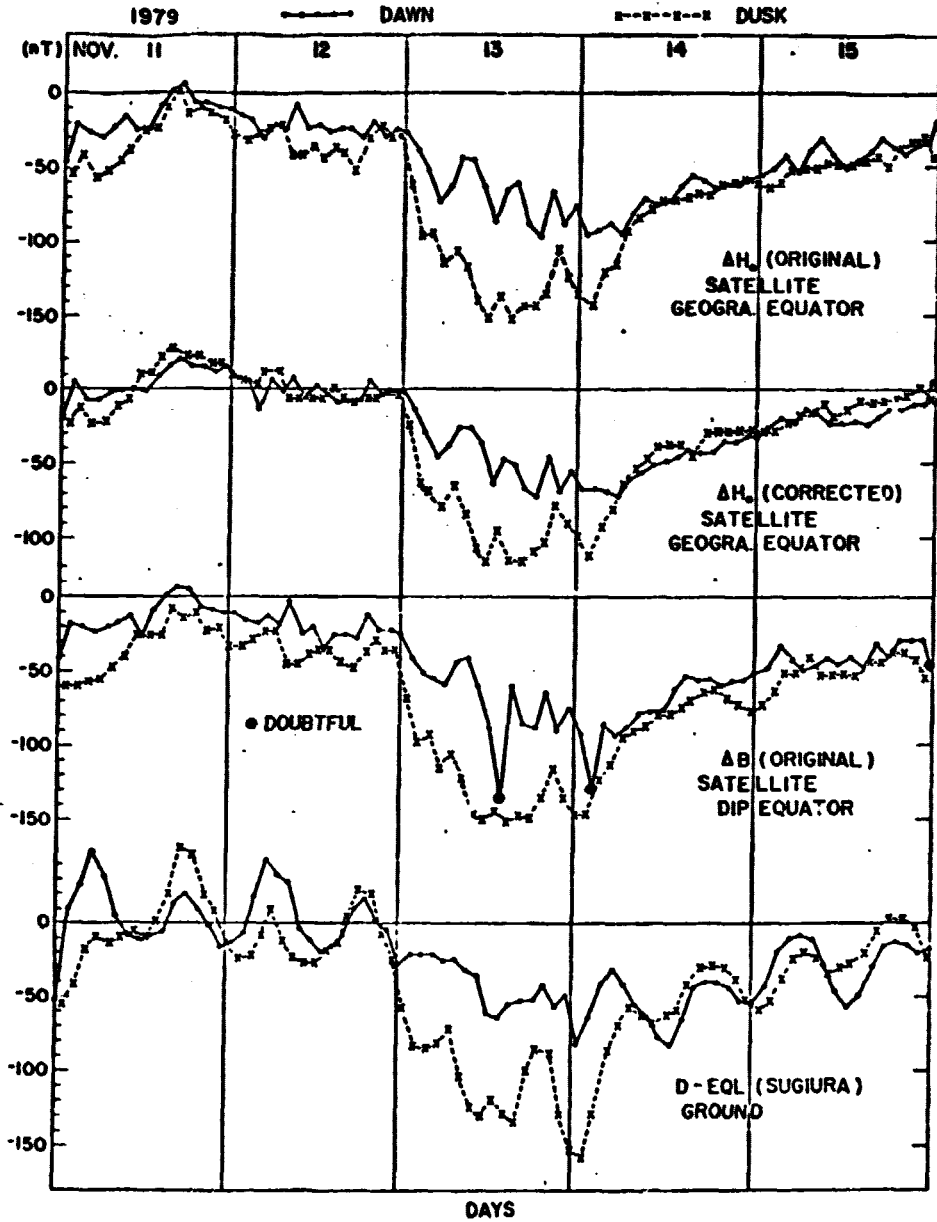


Fig. 1 - Plot of ΔH_0 (i.e. ΔH at equatorial crossing, original as well as corrected for base level), ΔB (total field at dip equator) and D-EQL (Equatorial disturbance index for ground), for Nov. 11-15, 1979 for Dawn (full lines) and Dusk (crosses and dashes).

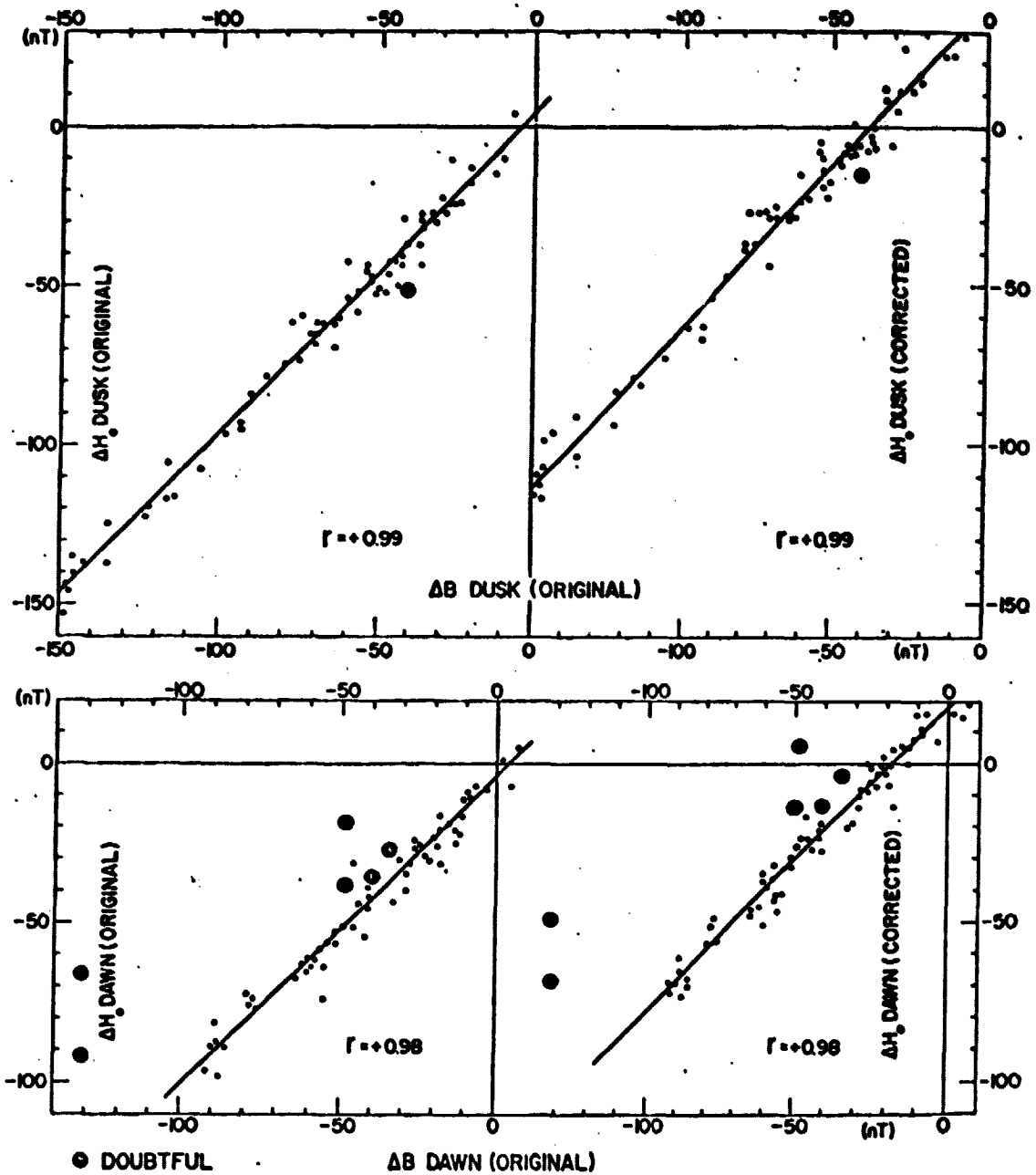


Fig. 2 - Upper half, ΔH_0 Dusk (original and corrected) versus ΔB Dusk (original). Lower half, ΔH_0 Dawn (original and corrected) versus ΔB Dawn (original).

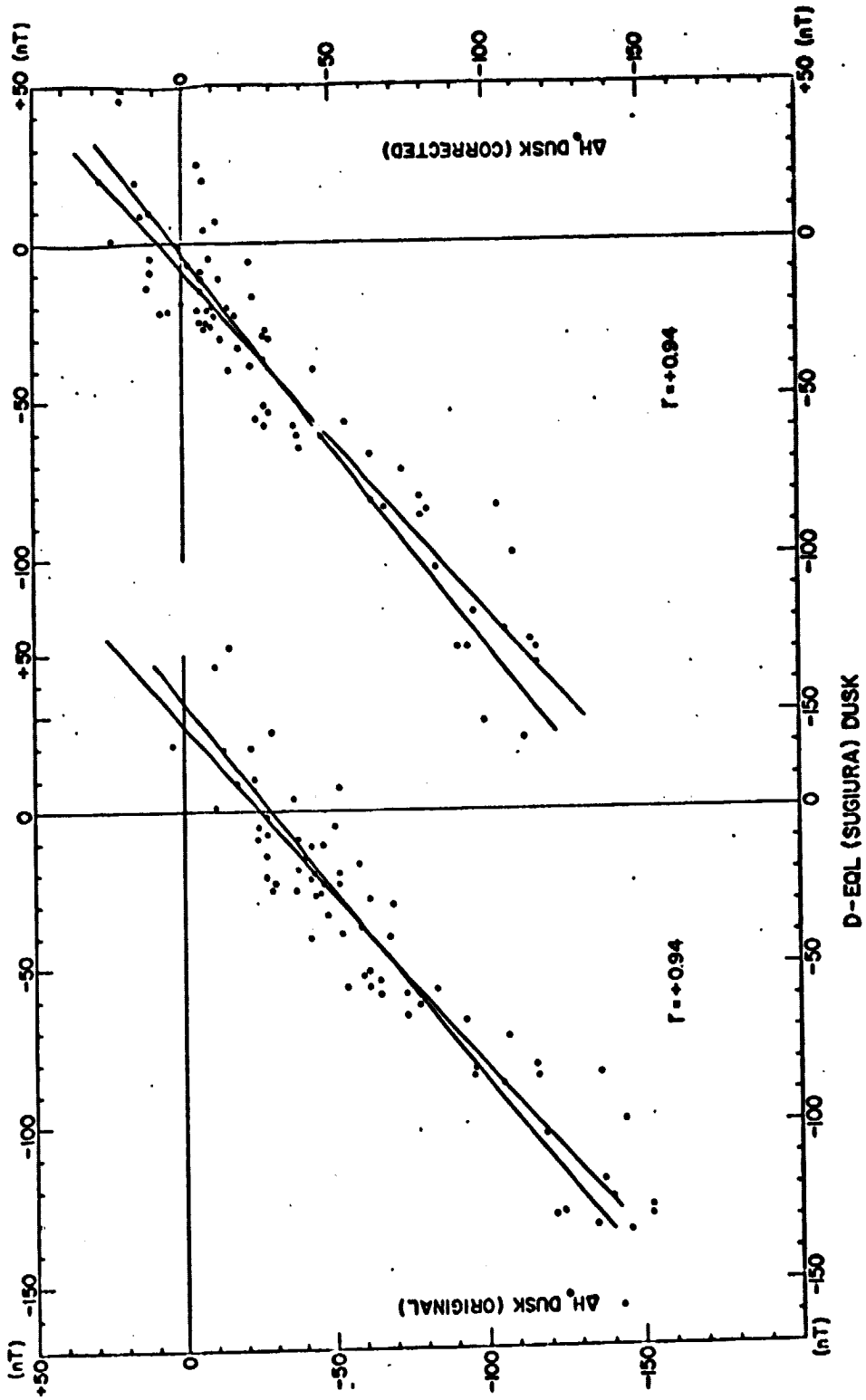
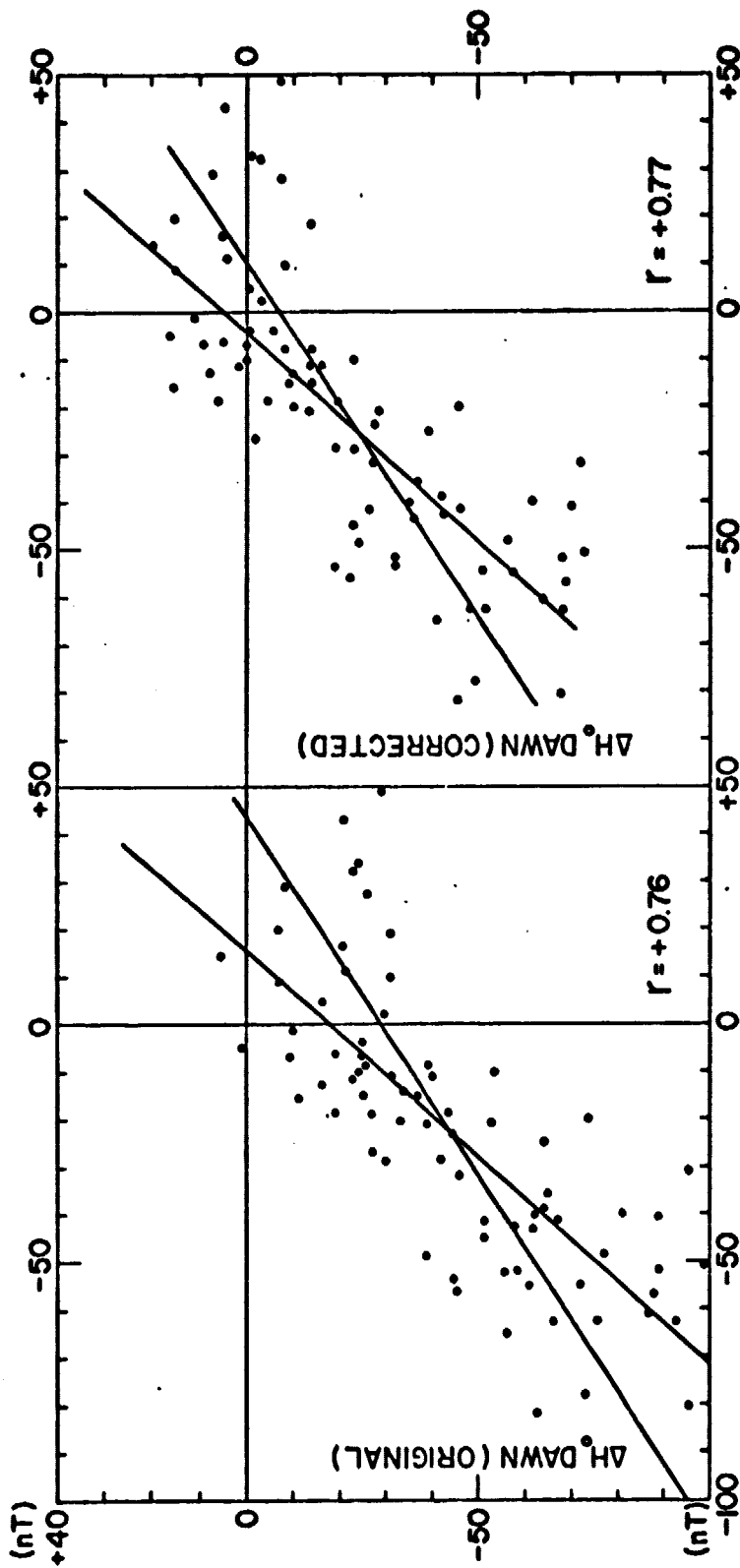


Fig. 3 - ΔH_0 Dusk (original and corrected) versus D-EOL Dusk (by Sugiura, for ground stations).
Regression lines for direct and reverse correlations are marked.



D-EQL (SUGIURA) DAWN

Fig. 4 - ΔH_0 Dawn (original and corrected) versus D-EQL Dawn (by Sugiura, for ground stations).
Regression lines for direct and reverse correlations are marked.

ORIGINAL PAGE IS
OF POOR QUALITY

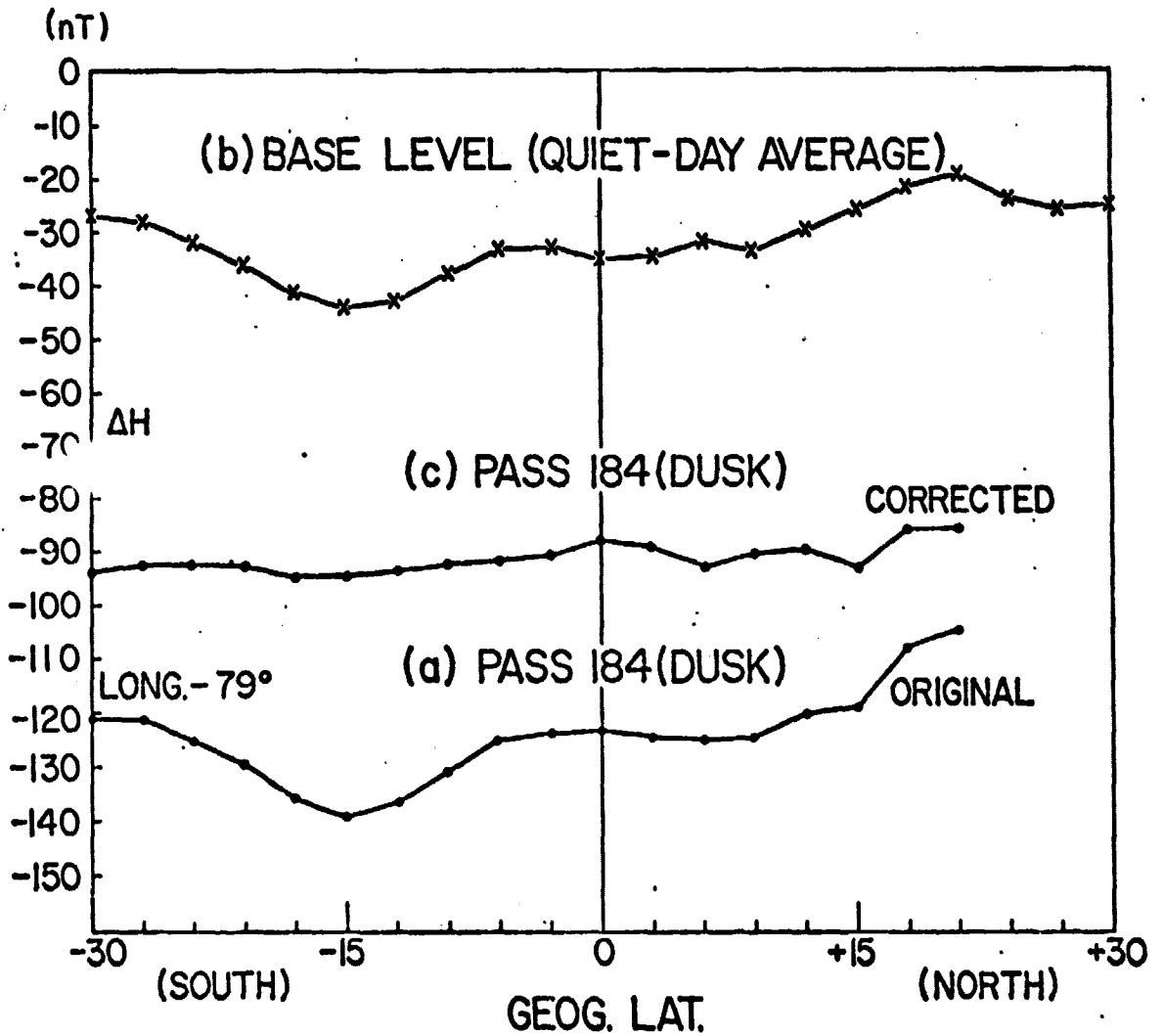


Fig. 5 - Latitudinal variation of ΔH for
(a) The specific disturbed-day Dusk pass No. 184 at longitude -79° .
(b) Quiet day base level obtained as average for six quiet-day passes in the longitude belt 75° - 80° W.
(c) The difference (a minus (b)).

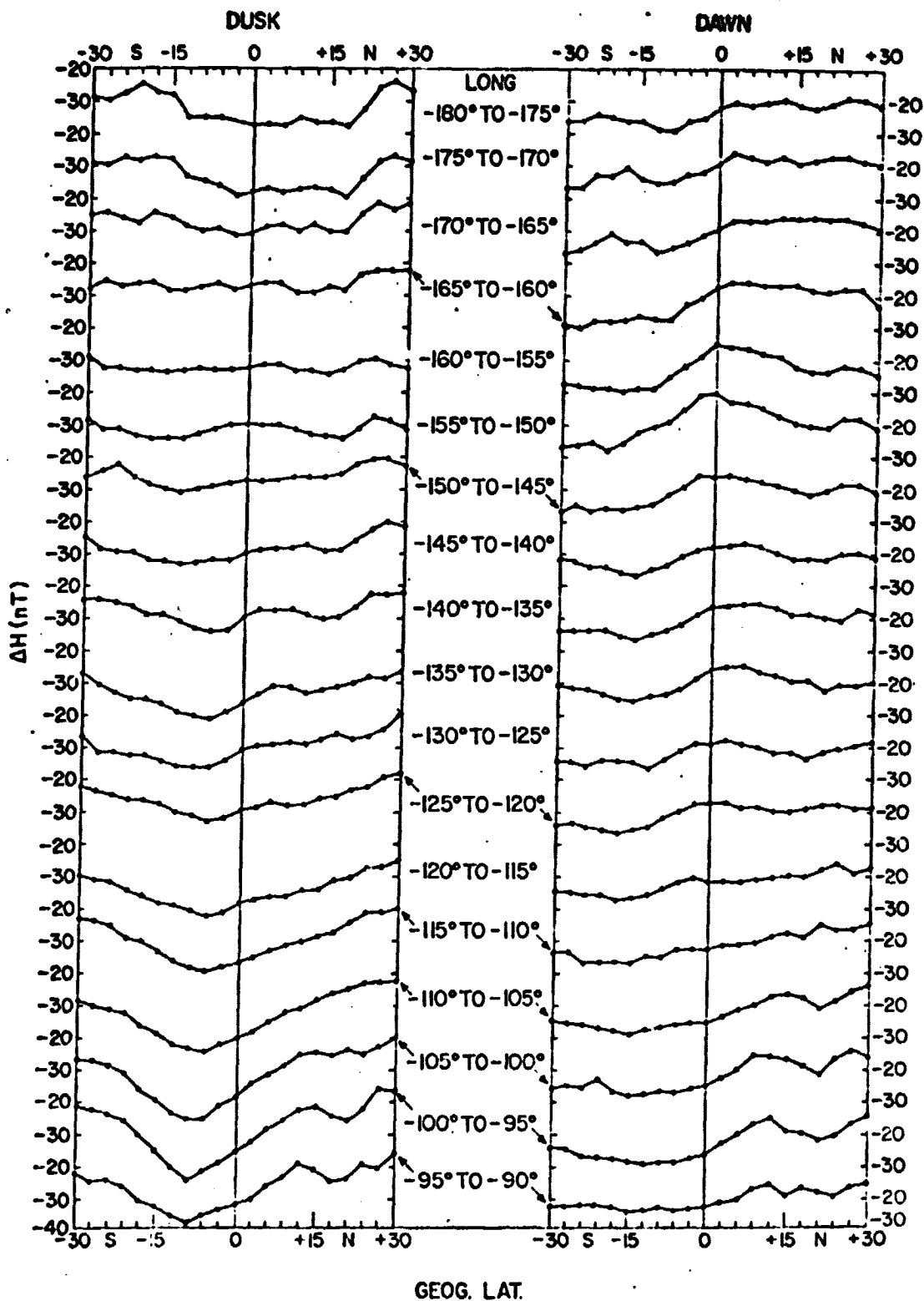


Fig. 6(a) - Average latitudinal patterns of ΔH (Dusk) (left half) and ΔH (Dawn) (right half) for successive 5° longitude belts for the longitude ranges, longitude -180° to -90°. + = East, - = West

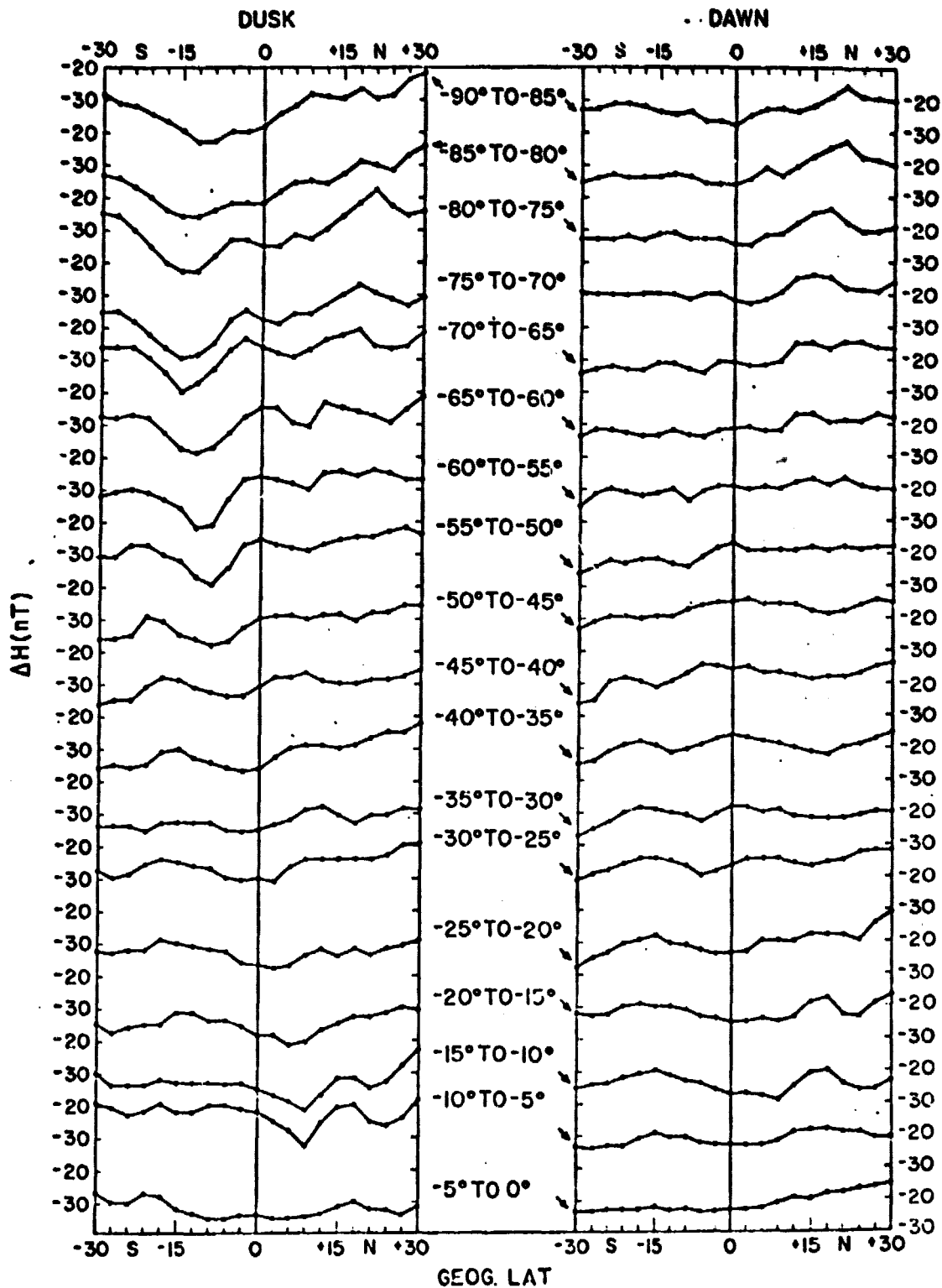


Fig. 6(b) - Average latitudinal patterns of ΔH (Dusk) (left half) and ΔH (Dawn) (right half) for successive 5° longitude belts for the longitude ranges, longitude -90° to 0° .
+ = East, - = West.

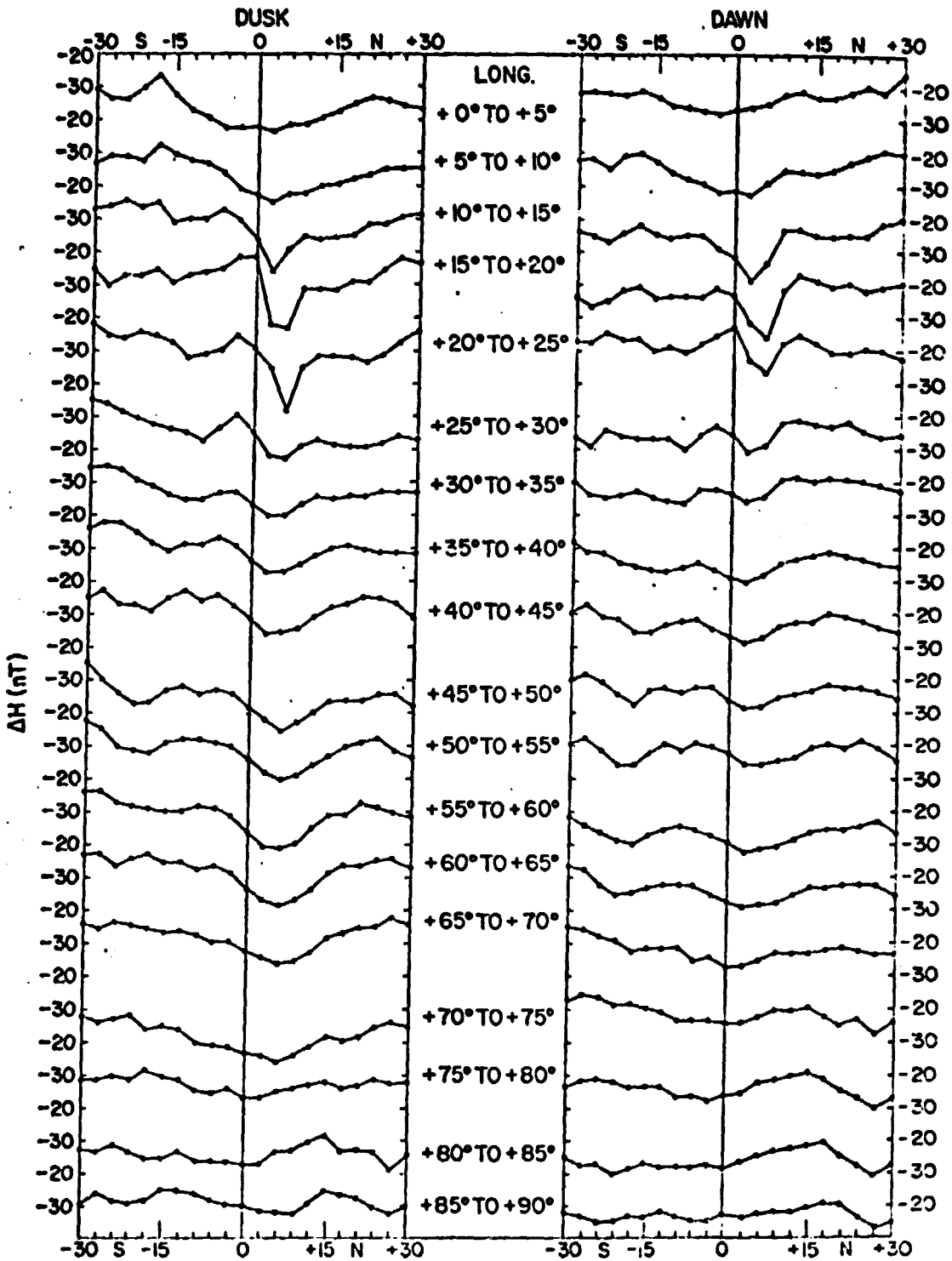


Fig. 6(c) - Average latitudinal patterns of ΔH (Dusk) (left half) and ΔH (Dawn) (right half) for successive 5° longitude belts for the longitude ranges, longitude 0° to 90°. + = East, - = West.

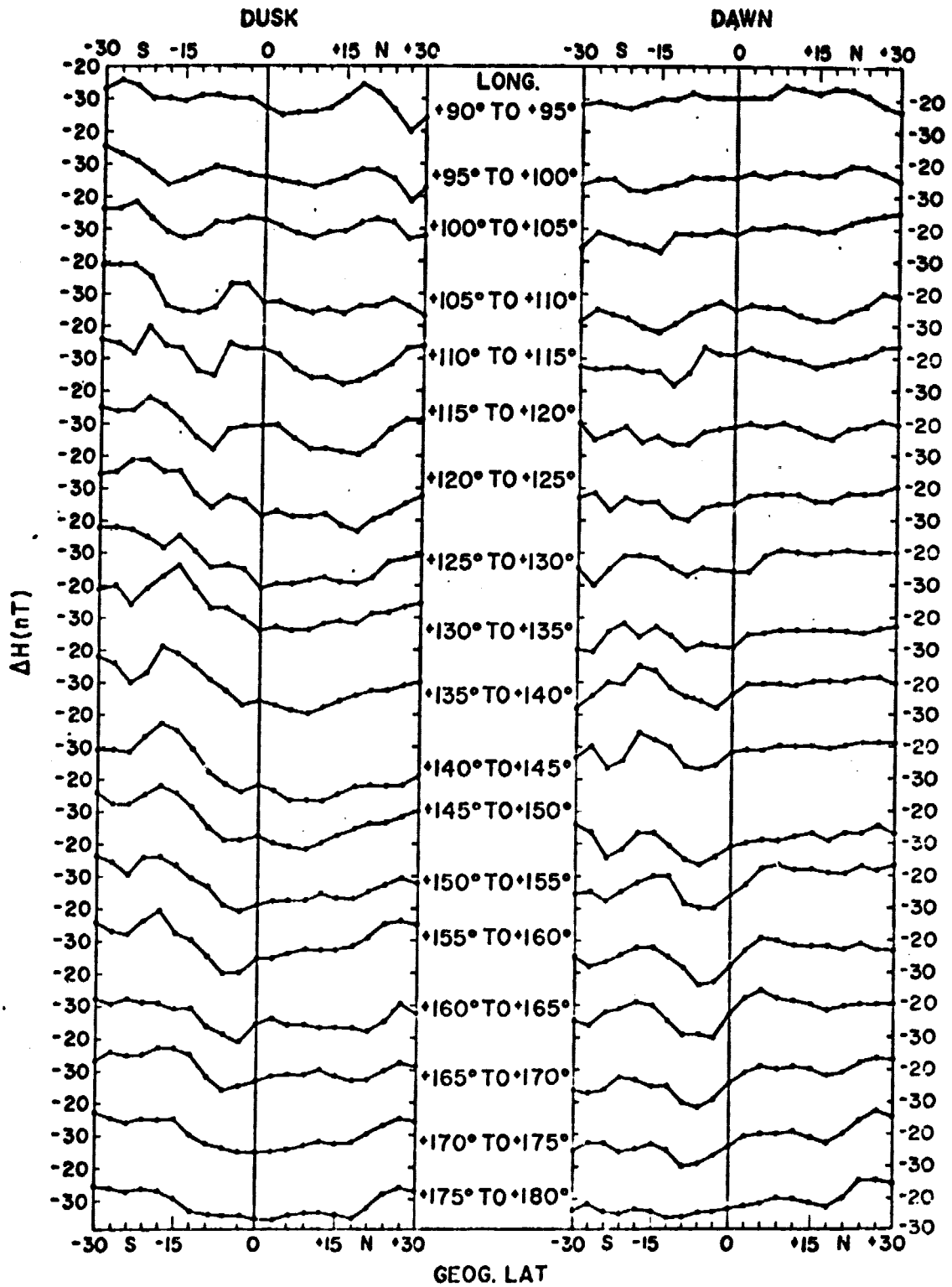


Fig. 6(d) - Average latitudinal patterns of ΔH (Dusk) (left half) and ΔH (Dawn) (right half) for successive 5° longitude belts for the longitude ranges, longitude +90° to +180°. + = East, - = West.

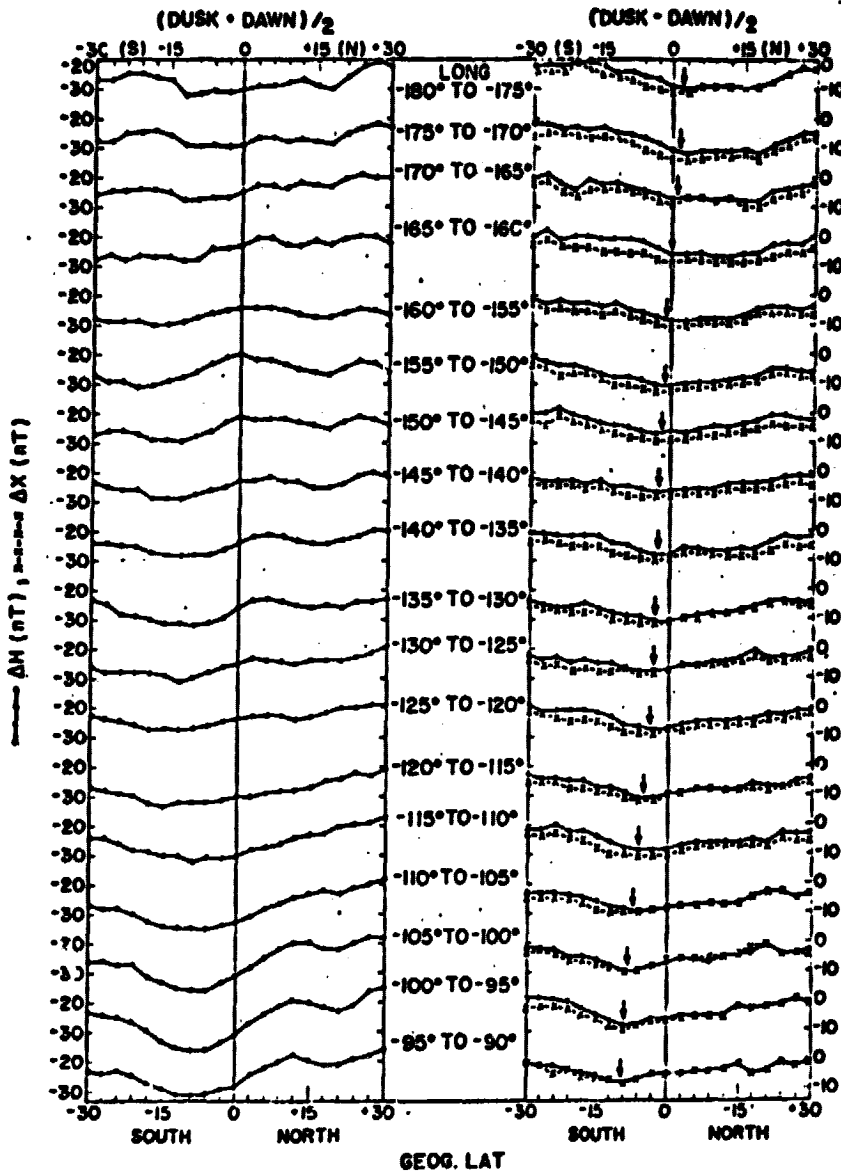


Fig. 7(a) - Average latitudinal variations for $\Delta H_{(Dusk+Dawn)/2}$ (left half) and $\Delta H_{(Dusk-Dawn)/2}$ (right half, full lines) for successive 5° longitude intervals for the longitude ranges, longitude -180° to -90°. In the right half, crosses and dashes represent the X component and vertical arrows indicate the position of the dip equator.

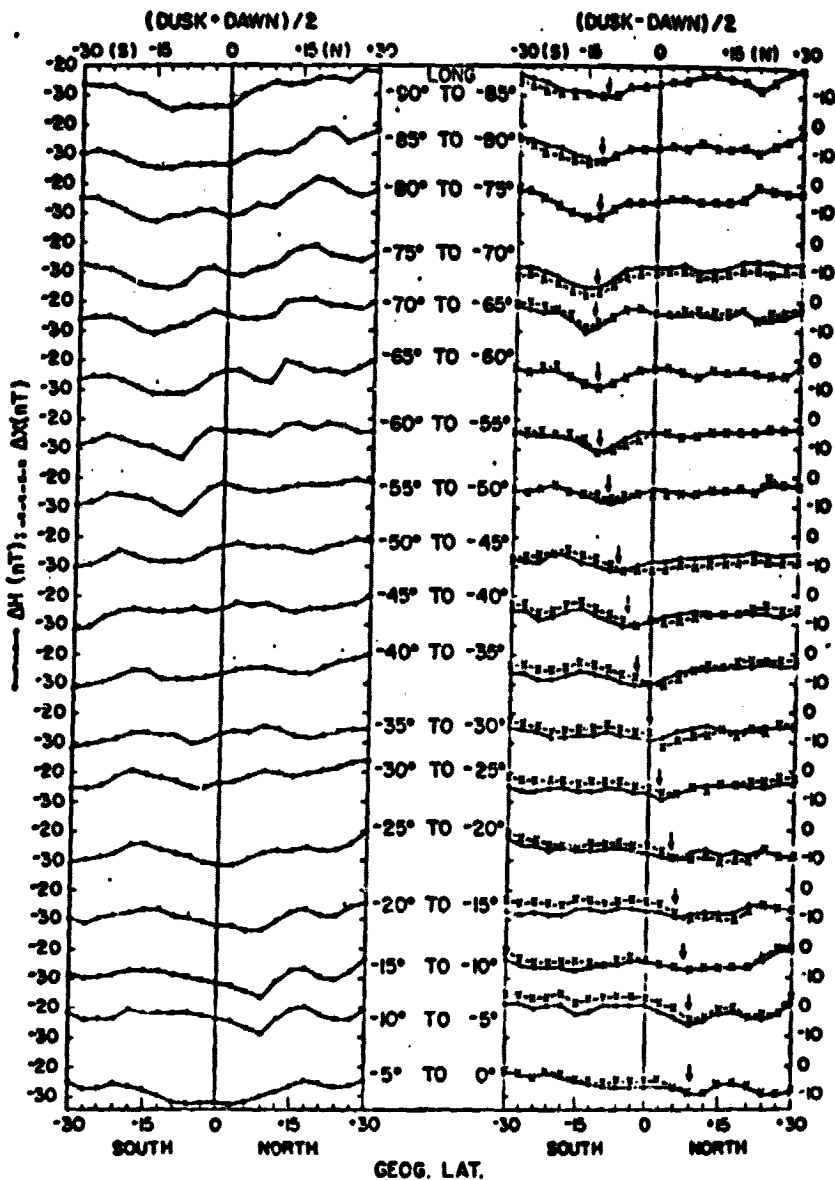


Fig. 7(b) - Average latitudinal variations for ΔH (Dusk+Dawn)/2 (left half) and ΔH (Dusk-Dawn)/2 (right half, full lines) for successive 5° longitude intervals for the longitude ranges, longitude -90° to 0° . In the right half, crosses and dashes represent the X component and vertical arrows indicate the position of the dip equator.

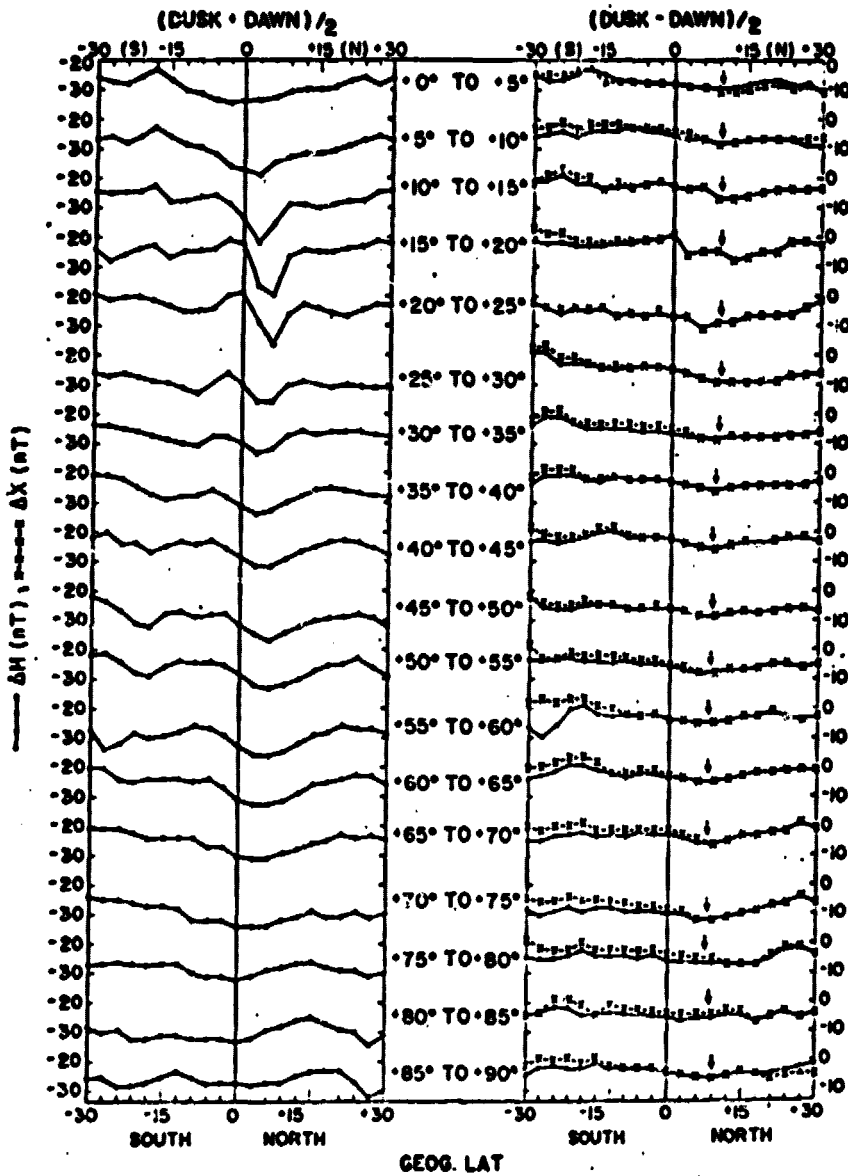


Fig. 7(c) - Average latitudinal variations for $\Delta H (Dusk+Dawn)/2$ (left half) and $\Delta H(Dusk-Dawn)/2$ (right half, full lines) for successive 5° longitude intervals for the longitude ranges, longitude 0° to $+90^\circ$. In the right half, crosses and dashes represent the X component and vertical arrows indicate the position of the dip equator.

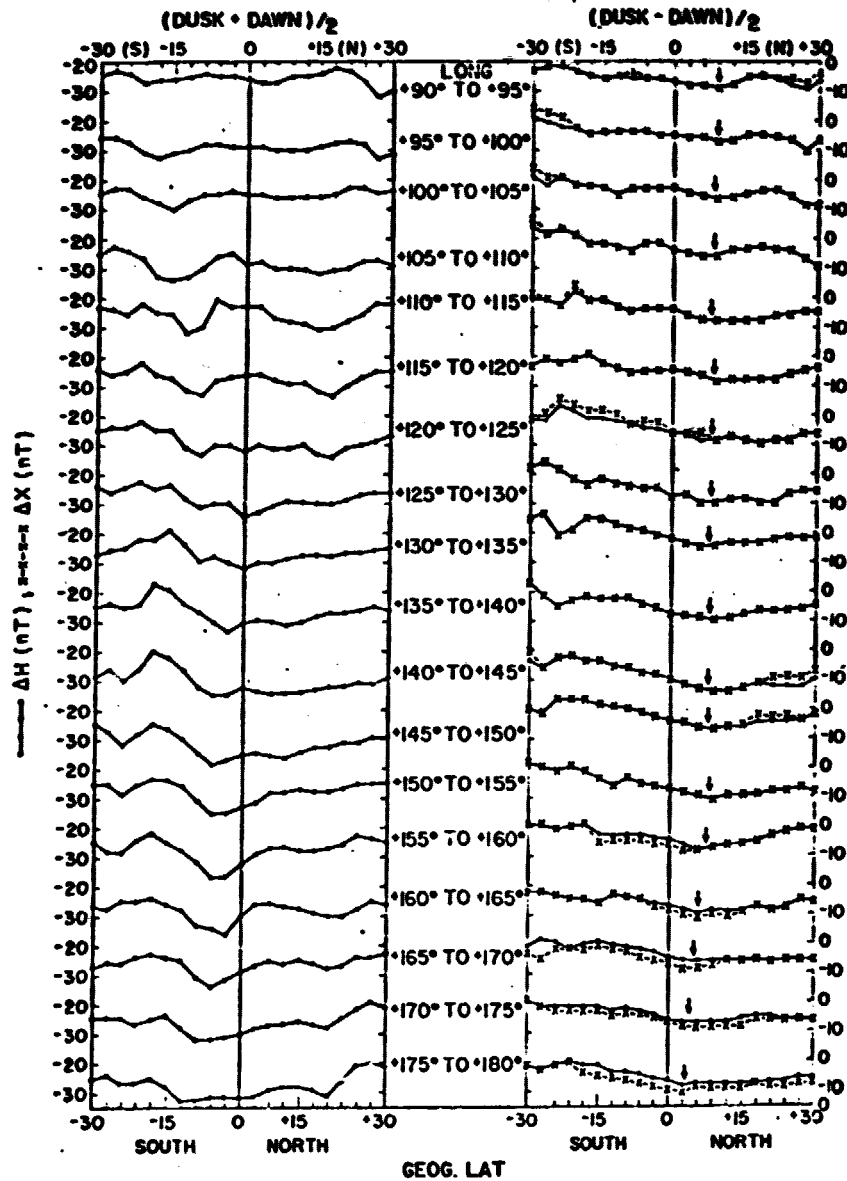


Fig. 7(d) - Average latitudinal variations for $\Delta H(\text{Dusk} + \text{Dawn})/2$ (left half) and $\Delta H(\text{Dusk} - \text{Dawn})/2$ (right half, full lines) for successive 5° longitude intervals for the longitude ranges, longitude $+90^\circ$ to $+180^\circ$. In the right half, crosses and dashes represent the X component and vertical arrows indicate the position of the dip equator.

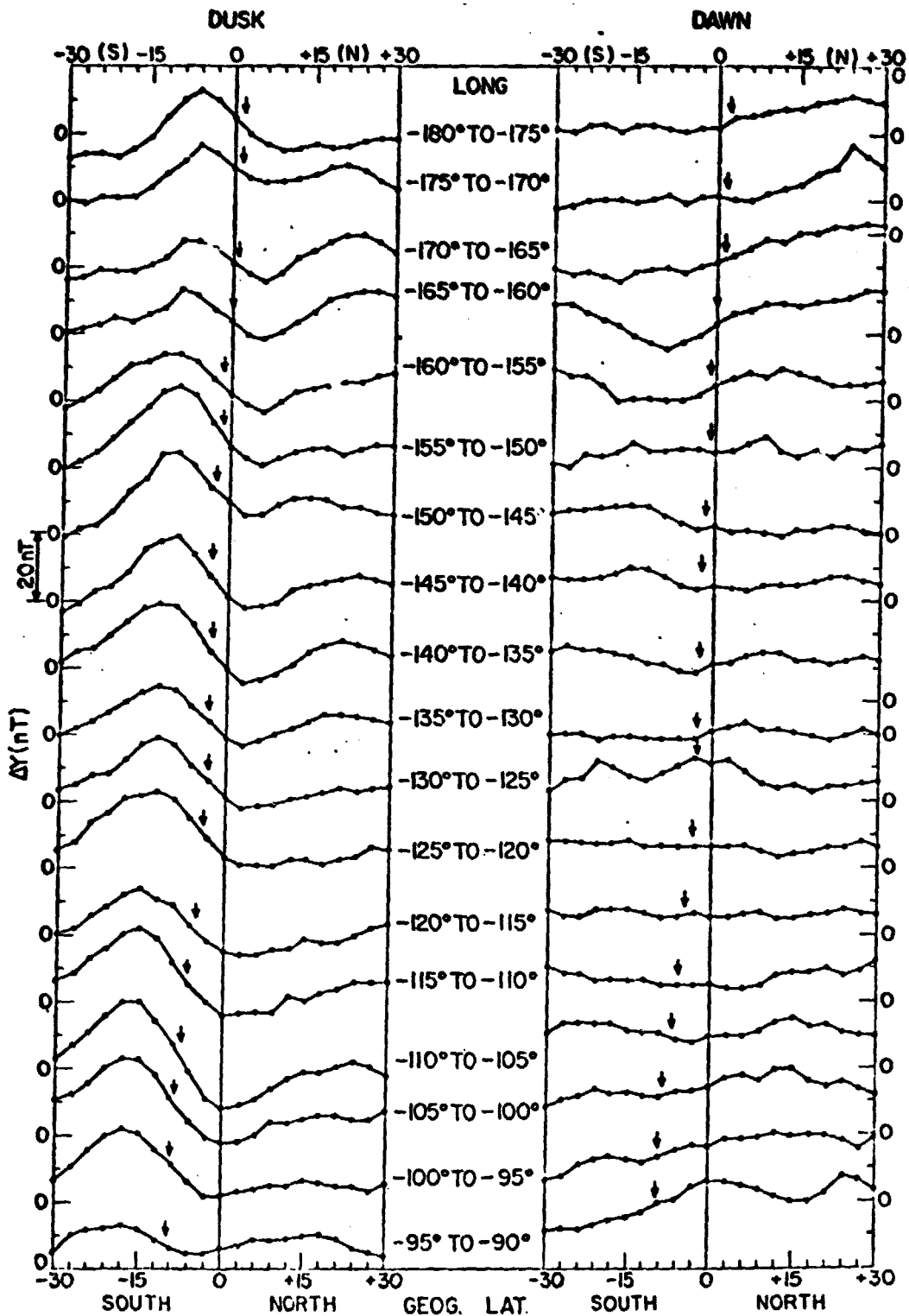


Fig. 8(a) - Average latitudinal variations for ΔY (Dusk) (left half) and ΔH (Dawn) (right half) for successive 5° longitude belts for the longitude ranges, longitude -180° to -90° . Vertical arrows indicate the position of the dip equator.

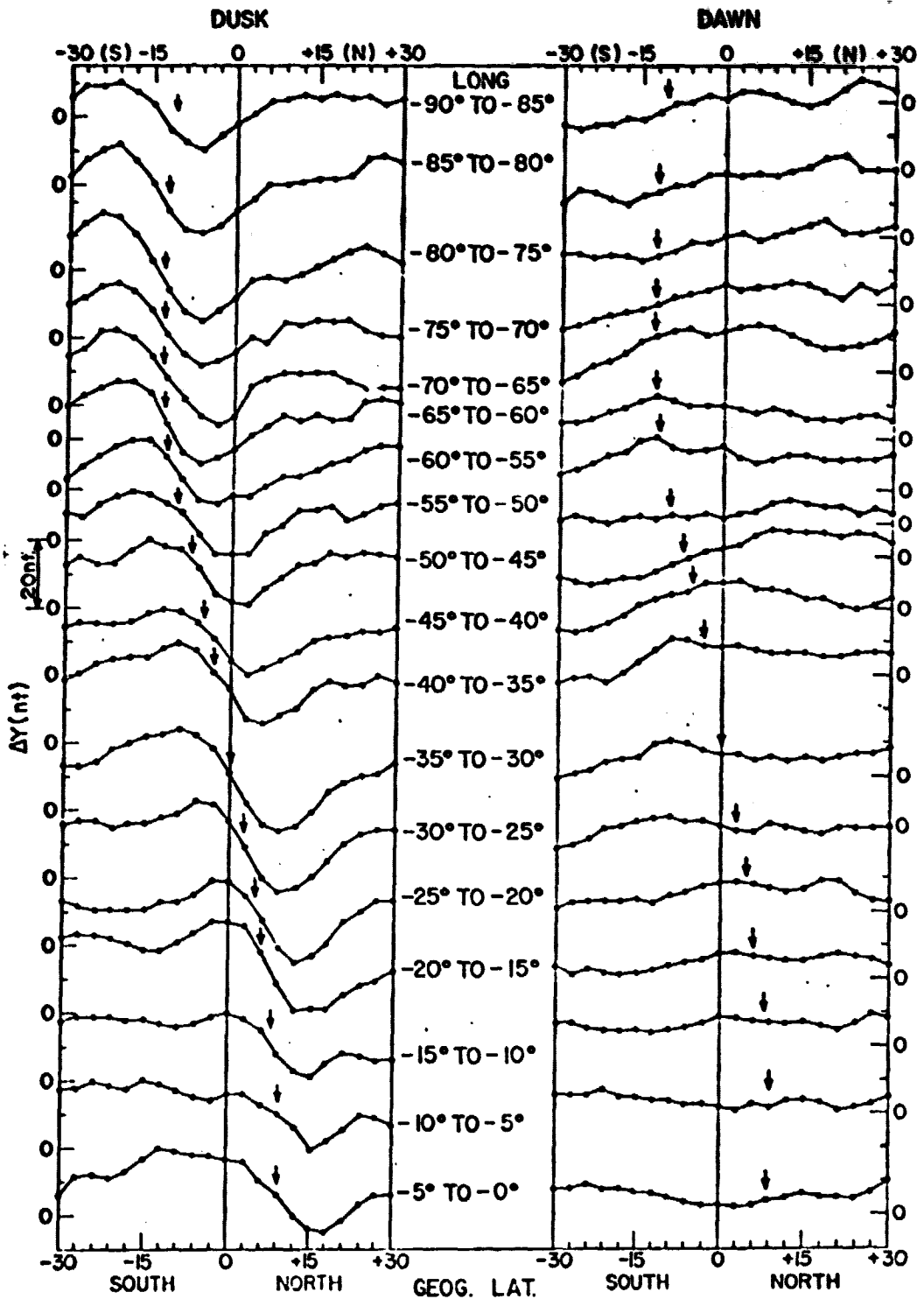


Fig. 8(b) - Average latitudinal variations for $\Delta Y(\text{Dusk})$ (left half) and $\Delta Y(\text{Dawn})$ (right half) for successive 5° longitude belts for the longitudes ranges, longitude -90° to 0° . Vertical arrows indicate the position of the dip equator.

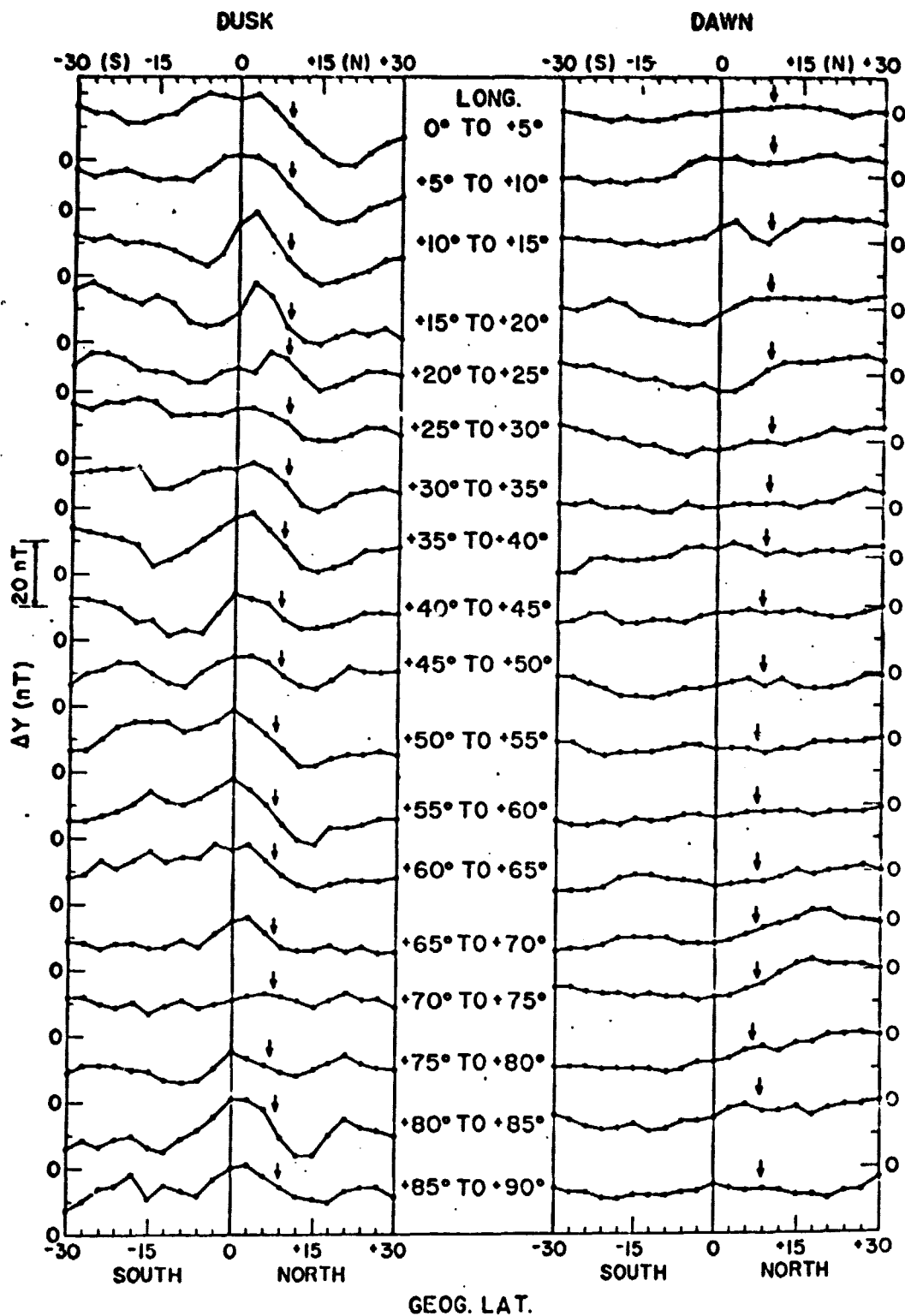


Fig. 8(c) - Average latitudinal variations for ΔY (Dusk) (left half) and ΔY (Dawn) (right half) for successive 5° longitude belts for the longitudes ranges, longitude 0° to +90°. Vertical arrows indicate the position of the dip equator.

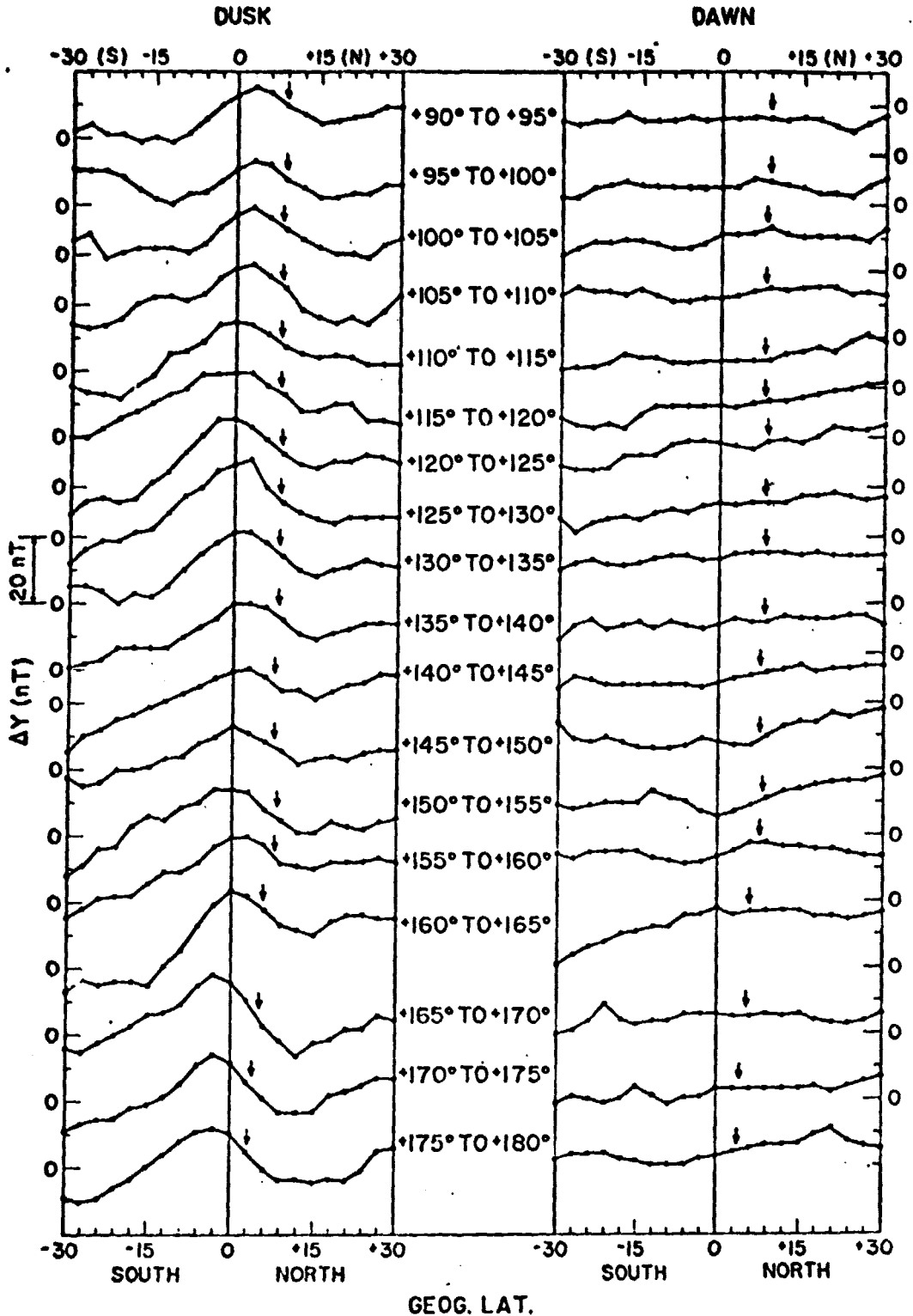


Fig. 8(d) - Average latitudinal variations for ΔY (Dusk) (left half) and ΔY (Dawn) (right half) for successive 5° longitude belts for the longitudes ranges, longitude +90° to +180°. Vertical arrows indicate the position of the dip equator.

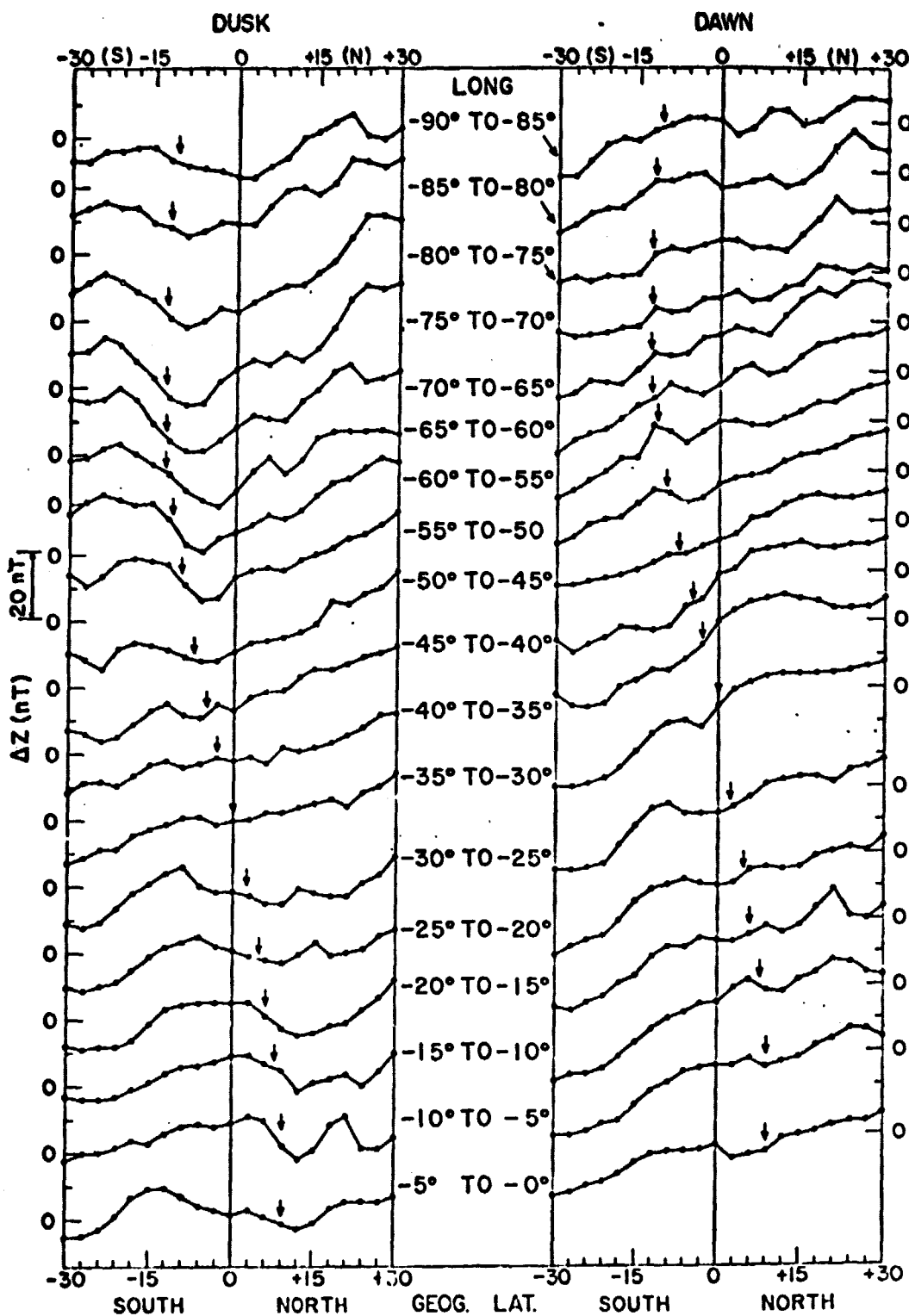


Fig. 9 - Average latitudinal variations for ΔZ (Dusk) (left half) and ΔZ (Dawn) (right half) for 5° longitude belts in the longitude range -90° to 0°, in which the position of the dip equator (vertical arrows) changes rapidly.

1963 10 10 10 30
Y 10 10 10 10 10

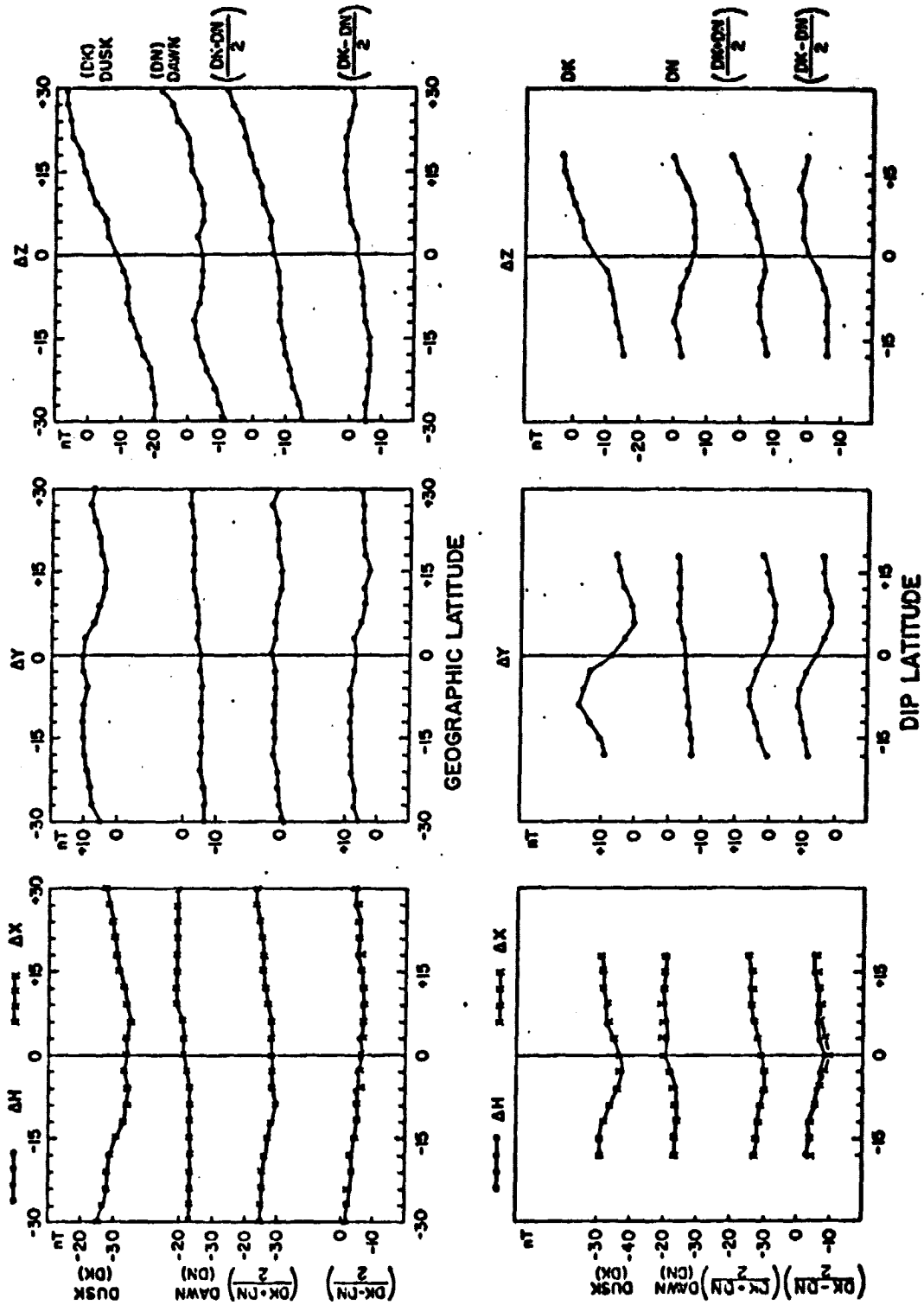


Fig. 11 - Average latitudinal variations for ΔH and ΔX (first column, full lines and crosses), ΔY (second column) and ΔZ (third column) for Dusk, Dawn, $(Dusk+Dawn)/2$, $(Dusk-Dawn)/2$. The upper half has abscissa as geographical latitude while the lower half has abscissa as dip latitude.

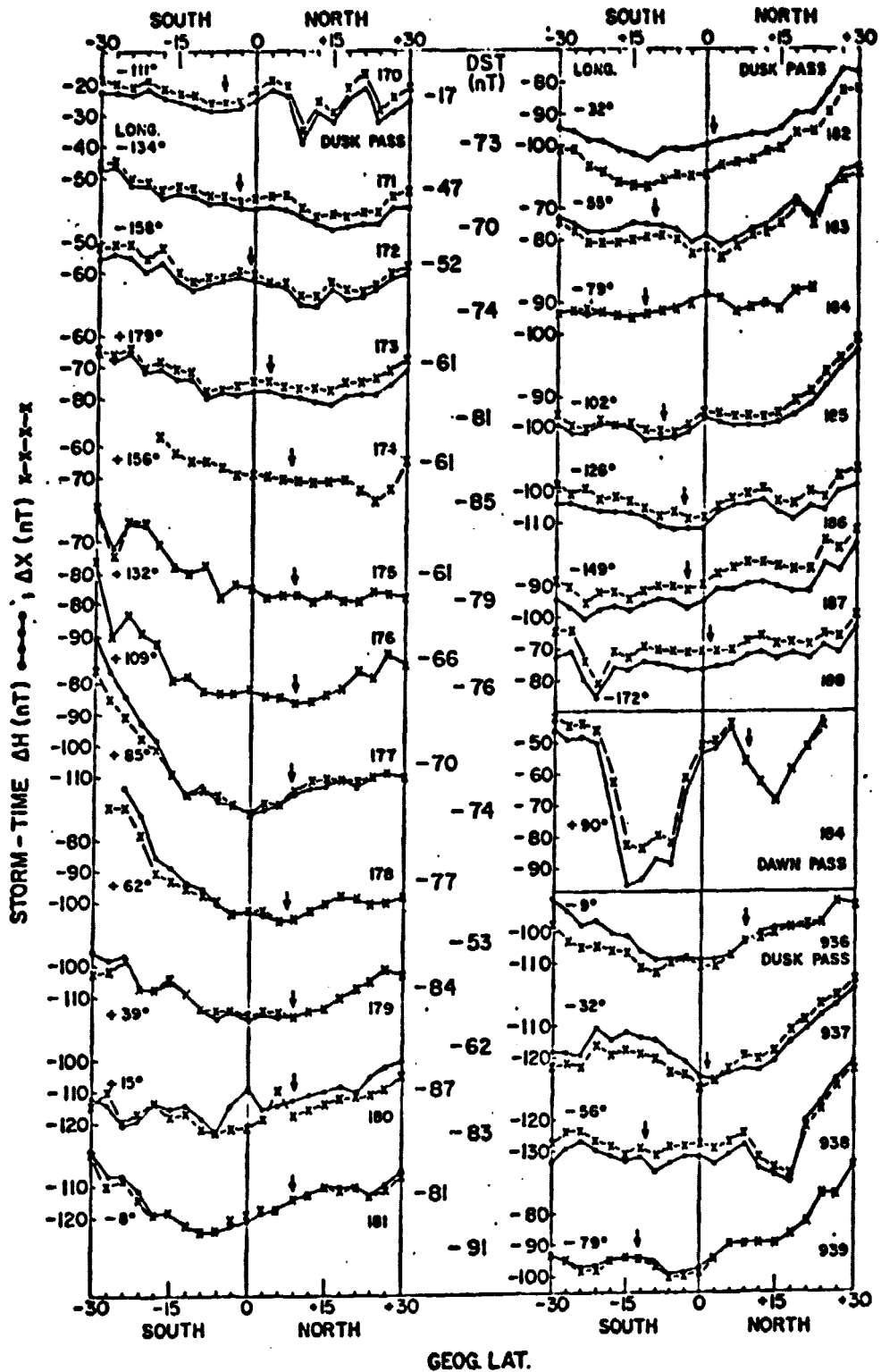


Fig. 12 - Latitudinal variation of ΔH (full lines) and ΔX (crosses and dashes) corrected for base levels, for the Dusk passes 170-188 during the storm of Nov. 11-15, 1979, as also for the Dawn pass 184 and for the Dusk passes 936-939 in Jan. 1980. The pass number, longitude and Dst are indicated for each pass. Vertical arrows indicate the position of the dip equator.

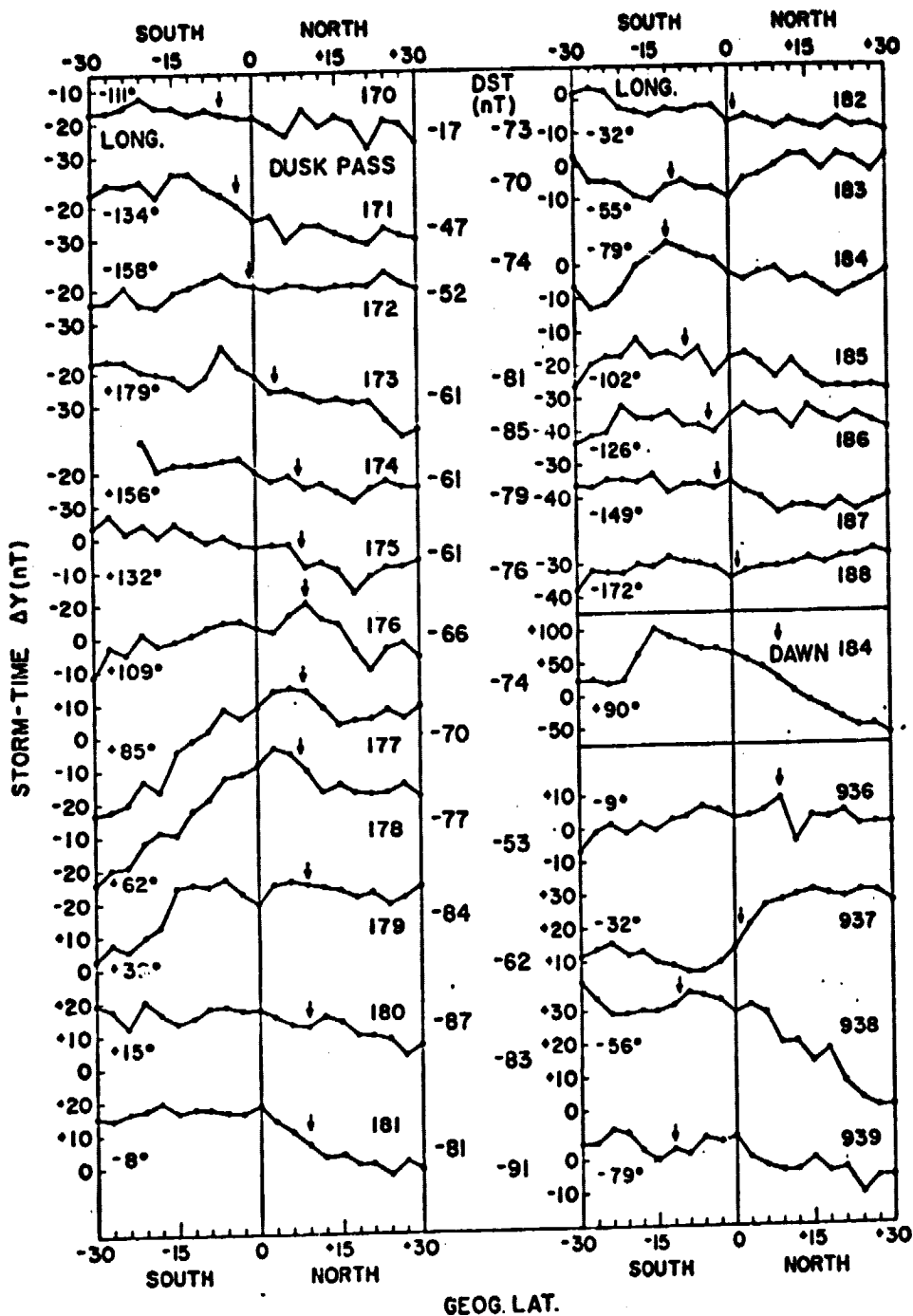


Fig. 13 - Same as Fig. 12, but for ΔY .

ORIGINAL PAGE IS
OF POOR QUALITY

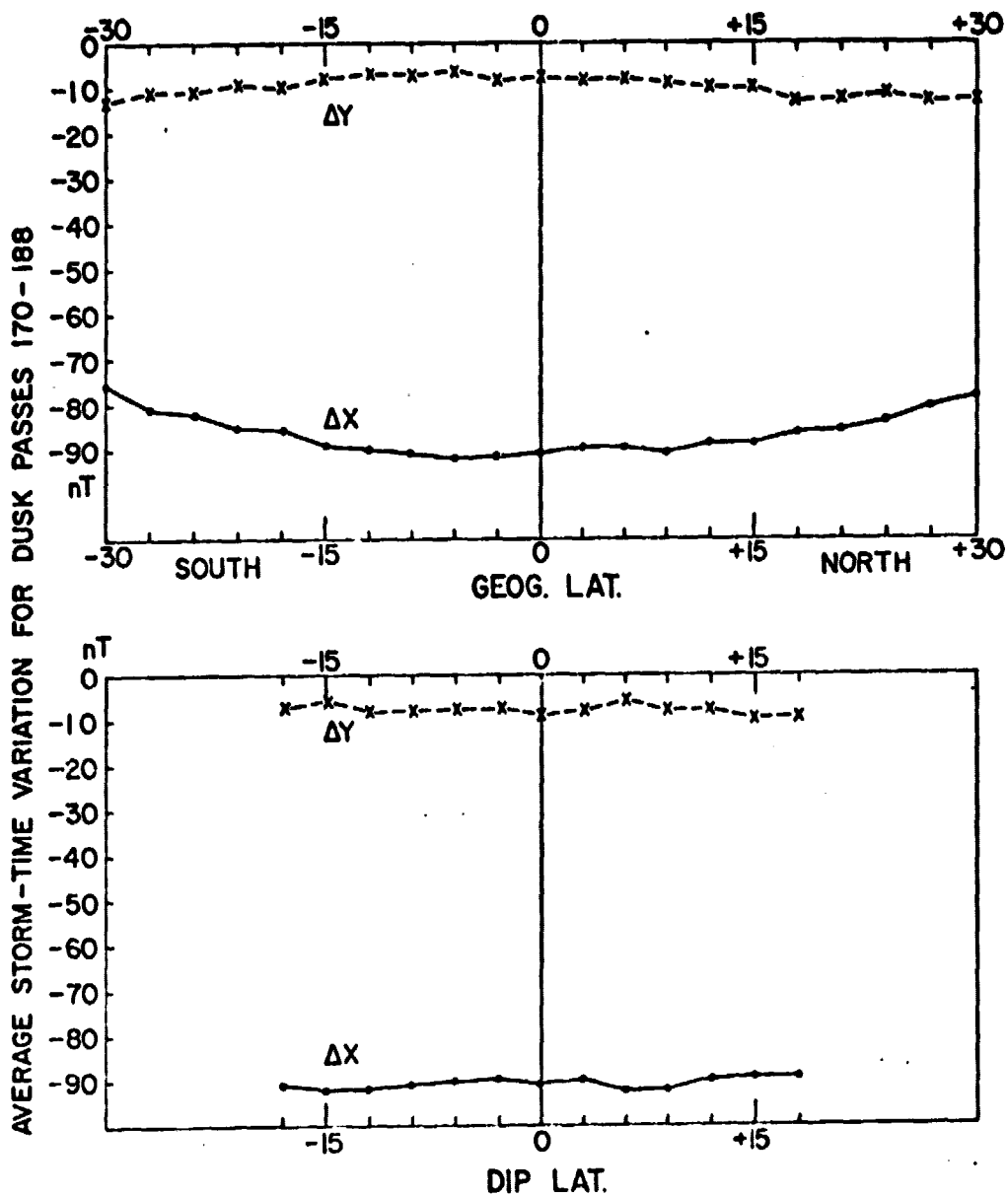


Fig. 14 - Average latitudinal distribution of ΔX and ΔY for the storm-time Dusk passes 170-188 on Nov. 13-14, 1979. Upper half - For geographical latitudes. Lower half - For dip latitudes.

ORIGINAL PAGE IS
OF POOR QUALITY

Table 1 - Erroneous values of Delta B as printed in Investigator B Table (pages 1-5, 1-6, 1-7 for passes 138 to 216 for Nov. 11-15, 1979) of the NASA Tech. Memorandum 82160 (Magsat Data Processing: A report for investigators, Langel et al., Nov. 1981).

DUSK (Ascending) Passes			DAWN (Descending) Passes		
Pass No	DELTA B		Pass No	DELTA B	
	As given	Should be about		As given	Should be about
198	+20.9	-69	162	- 35.1	-27
205	-40.2	-53	168	- 21.6	-26
			178	-136.0	-66
			186	-132.0	-82
			204	- 49.1	-38
			205	- 46.3	No data (?)
			209	- 47.2	No data
			211	- 40.4	-36
			215	- 48.9	-16

Table 5: ΔH (Dusk - Dawn)/2, units nT.

MAGNETIC RANGE	LATITUDE FROM																DEGREES					
	-30	-27	-24	-21	-18	-15	-12	-9	-6	-3	0	+3	+6	+9	+12	+15	+18	+21	+24	+27	+30	
170 TO 175	-2	-2	-2	-1	+1	+2	+4	+4	+6	+7	+8	+8	+10	+10	+9	+8	+6	+7	+5	+3	+2	+2
175 TO 170	-2	-2	-2	-3	+4	+3	+4	+3	+4	+7	+6	+6	+11	+17	+11	+11	+8	+9	+7	+5	+5	+5
170 TO 165	0	1	-2	+4	+1	-2	+7	+3	+4	+4	+9	+9	+9	+7	+7	+6	+6	+6	+6	+3	+3	+2
165 TO 160	0	2	+1	0	0	-1	-1	-1	-2	-2	-2	-2	-2	-2	-2	-2	-2	-2	-2	-2	-2	-2
160 TO 155	-1	-3	+2	+3	+3	+3	+3	+3	+3	+3	+3	+3	+3	+3	+3	+3	+3	+3	+3	+3	+3	+3
155 TO 150	-1	-3	+4	+4	+5	+7	+8	+8	+9	+11	+11	+12	+10	+10	+9	+8	+6	+7	+5	+5	+4	+4
150 TO 145	0	0	2	+1	+2	+3	+4	+5	+6	+7	+8	+8	+7	+6	+5	+4	+3	+2	+1	+1	+1	+1
145 TO 140	+2	+3	+3	+3	+4	+5	+5	+6	+7	+8	+8	+7	+6	+5	+4	+3	+2	+1	+1	+1	+1	+1
140 TO 135	-1	-1	-2	-2	-2	-2	-2	-2	-2	-2	-2	-2	-2	-2	-2	-2	-2	-2	-2	-2	-2	-2
135 TO 130	+4	+5	+4	+6	+5	+6	+8	+8	+9	+11	+11	+12	+9	+8	+7	+6	+4	+5	+3	+3	+3	+3
130 TO 125	-2	-4	-3	+5	+4	-5	-5	-7	-9	-9	-11	-11	-8	-8	-8	-8	-8	-8	-8	-8	-8	-8
125 TO 120	1	-1	-1	-1	-1	-2	-3	-4	-7	-7	-7	-7	-6	-5	-5	-5	-5	-5	-5	-5	-5	-5
120 TO 115	-3	-4	-4	+5	-5	-7	-7	-7	-7	-7	-7	-7	-7	-7	-7	-7	-7	-7	-7	-7	-7	-7
115 TO 110	-1	-1	0	-2	-2	-4	-4	-4	-4	-4	-4	-4	-4	-4	-4	-4	-4	-4	-4	-4	-4	-4
110 TO 105	-3	-3	0	+2	+5	-6	-8	-8	-10	-10	-10	-10	-10	-10	-10	-10	-10	-10	-10	-10	-10	-10
105 TO 100	-1	-2	+2	+3	+5	+6	+8	+8	+10	+10	+10	+10	+10	+10	+10	+10	+10	+10	+10	+10	+10	+10
100 TO 95	1	1	1	1	0	+2	+4	+4	+4	+4	+4	+4	+4	+4	+4	+4	+4	+4	+4	+4	+4	+4
95 TO 90	-1	-2	+2	+3	+4	+5	+7	+7	+8	+8	+8	+8	+8	+8	+8	+8	+8	+8	+8	+8	+8	+8
90 TO 85	+3	+4	+6	+8	+8	+9	+10	+10	+10	+10	+10	+10	+10	+10	+10	+10	+10	+10	+10	+10	+10	+10
85 TO 80	-4	-5	+7	+7	+8	+9	+10	+10	+10	+10	+10	+10	+10	+10	+10	+10	+10	+10	+10	+10	+10	+10
80 TO 75	-2	-2	+4	+4	+5	+6	+6	+6	+6	+6	+6	+6	+6	+6	+6	+6	+6	+6	+6	+6	+6	+6
75 TO 70	-4	-4	+5	+5	+6	+6	+6	+6	+6	+6	+6	+6	+6	+6	+6	+6	+6	+6	+6	+6	+6	+6
70 TO 65	-4	-4	+5	+5	+6	+6	+6	+6	+6	+6	+6	+6	+6	+6	+6	+6	+6	+6	+6	+6	+6	+6
65 TO 60	-4	-4	+5	+5	+6	+6	+6	+6	+6	+6	+6	+6	+6	+6	+6	+6	+6	+6	+6	+6	+6	+6
60 TO 55	-4	-4	+5	+5	+6	+6	+6	+6	+6	+6	+6	+6	+6	+6	+6	+6	+6	+6	+6	+6	+6	+6
55 TO 50	-4	-4	+5	+5	+6	+6	+6	+6	+6	+6	+6	+6	+6	+6	+6	+6	+6	+6	+6	+6	+6	+6
50 TO 45	-4	-4	+5	+5	+6	+6	+6	+6	+6	+6	+6	+6	+6	+6	+6	+6	+6	+6	+6	+6	+6	+6
45 TO 40	-5	-5	+6	+6	+7	+7	+7	+7	+7	+7	+7	+7	+7	+7	+7	+7	+7	+7	+7	+7	+7	+7
40 TO 35	-6	-6	+6	+6	+7	+7	+7	+7	+7	+7	+7	+7	+7	+7	+7	+7	+7	+7	+7	+7	+7	+7
35 TO 30	-6	-6	+6	+6	+7	+7	+7	+7	+7	+7	+7	+7	+7	+7	+7	+7	+7	+7	+7	+7	+7	+7
30 TO 25	-6	-6	+6	+6	+7	+7	+7	+7	+7	+7	+7	+7	+7	+7	+7	+7	+7	+7	+7	+7	+7	+7
25 TO 20	-6	-6	+6	+6	+7	+7	+7	+7	+7	+7	+7	+7	+7	+7	+7	+7	+7	+7	+7	+7	+7	+7
20 TO 15	-6	-6	+6	+6	+7	+7	+7	+7	+7	+7	+7	+7	+7	+7	+7	+7	+7	+7	+7	+7	+7	+7
15 TO 10	-6	-6	+6	+6	+7	+7	+7	+7	+7	+7	+7	+7	+7	+7	+7	+7	+7	+7	+7	+7	+7	+7
10 TO 5	-6	-6	+6	+6	+7	+7	+7	+7	+7	+7	+7	+7	+7	+7	+7	+7	+7	+7	+7	+7	+7	+7
5 TO 0	-6	-6	+6	+6	+7	+7	+7	+7	+7	+7	+7	+7	+7	+7	+7	+7	+7	+7	+7	+7	+7	+7
0 TO -5	-6	-6	+6	+6	+7	+7	+7	+7	+7	+7	+7	+7	+7	+7	+7	+7	+7	+7	+7	+7	+7	+7
-5 TO -10	-6	-6	+6	+6	+7	+7	+7	+7	+7	+7	+7	+7	+7	+7	+7	+7	+7	+7	+7	+7	+7	+7
-10 TO -15	-6	-6	+6	+6	+7	+7	+7	+7	+7	+7	+7	+7	+7	+7	+7	+7	+7	+7	+7	+7	+7	+7
-15 TO -20	-6	-6	+6	+6	+7	+7	+7	+7	+7	+7	+7	+7	+7	+7	+7	+7	+7	+7	+7	+7	+7	+7
-20 TO -25	-6	-6	+6	+6	+7	+7	+7	+7	+7	+7	+7	+7	+7	+7	+7	+7	+7	+7	+7	+7	+7	+7
-25 TO -30	-6	-6	+6	+6	+7	+7	+7	+7	+7	+7	+7	+7	+7	+7	+7	+7	+7	+7	+7	+7	+7	+7

(ΔH) (DUSK-DAWN)/2

Table 16: ΔZ (Dusk + Dawn)/2, units nT.

LATITUDE		LONGITUDE															
RANGE		10	27	54	81	108	135	162	189	216	243	270	297	324	351	378	405
100	10	17	14	11	8	5	2	-1	-4	-7	-10	-13	-16	-19	-22	-25	-28
100	20	16	13	10	7	4	1	-2	-5	-8	-11	-14	-17	-20	-23	-26	-29
100	30	15	12	9	6	3	0	-3	-6	-9	-12	-15	-18	-21	-24	-27	-30
100	40	14	11	8	5	2	-1	-4	-7	-10	-13	-16	-19	-22	-25	-28	-31
100	50	13	10	7	4	1	-2	-5	-8	-11	-14	-17	-20	-23	-26	-29	-32
100	60	12	9	6	3	0	-3	-6	-9	-12	-15	-18	-21	-24	-27	-30	-33
100	70	11	8	5	2	-1	-4	-7	-10	-13	-16	-19	-22	-25	-28	-31	-34
100	80	10	7	4	1	-2	-5	-8	-11	-14	-17	-20	-23	-26	-29	-32	-35
100	90	9	6	3	0	-3	-6	-9	-12	-15	-18	-21	-24	-27	-30	-33	-36
100	100	8	5	2	-1	-4	-7	-10	-13	-16	-19	-22	-25	-28	-31	-34	-37
100	110	7	4	1	-2	-5	-8	-11	-14	-17	-20	-23	-26	-29	-32	-35	-38
100	120	6	3	0	-3	-6	-9	-12	-15	-18	-21	-24	-27	-30	-33	-36	-39
100	130	5	2	-1	-4	-7	-10	-13	-16	-19	-22	-25	-28	-31	-34	-37	-40
100	140	4	1	-2	-5	-8	-11	-14	-17	-20	-23	-26	-29	-32	-35	-38	-41
100	150	3	0	-3	-6	-9	-12	-15	-18	-21	-24	-27	-30	-33	-36	-39	-42
100	160	2	-1	-4	-7	-10	-13	-16	-19	-22	-25	-28	-31	-34	-37	-40	-43
100	170	1	-2	-5	-8	-11	-14	-17	-20	-23	-26	-29	-32	-35	-38	-41	-44
100	180	0	-3	-6	-9	-12	-15	-18	-21	-24	-27	-30	-33	-36	-39	-42	-45
100	190	-1	-4	-7	-10	-13	-16	-19	-22	-25	-28	-31	-34	-37	-40	-43	-46
100	200	-2	-5	-8	-11	-14	-17	-20	-23	-26	-29	-32	-35	-38	-41	-44	-47
100	210	-3	-6	-9	-12	-15	-18	-21	-24	-27	-30	-33	-36	-39	-42	-45	-48
100	220	-4	-7	-10	-13	-16	-19	-22	-25	-28	-31	-34	-37	-40	-43	-46	-49
100	230	-5	-8	-11	-14	-17	-20	-23	-26	-29	-32	-35	-38	-41	-44	-47	-50
100	240	-6	-9	-12	-15	-18	-21	-24	-27	-30	-33	-36	-39	-42	-45	-48	-51
100	250	-7	-10	-13	-16	-19	-22	-25	-28	-31	-34	-37	-40	-43	-46	-49	-52
100	260	-8	-11	-14	-17	-20	-23	-26	-29	-32	-35	-38	-41	-44	-47	-50	-53
100	270	-9	-12	-15	-18	-21	-24	-27	-30	-33	-36	-39	-42	-45	-48	-51	-54
100	280	-10	-13	-16	-19	-22	-25	-28	-31	-34	-37	-40	-43	-46	-49	-52	-55
100	290	-11	-14	-17	-20	-23	-26	-29	-32	-35	-38	-41	-44	-47	-50	-53	-56
100	300	-12	-15	-18	-21	-24	-27	-30	-33	-36	-39	-42	-45	-48	-51	-54	-57
100	310	-13	-16	-19	-22	-25	-28	-31	-34	-37	-40	-43	-46	-49	-52	-55	-58
100	320	-14	-17	-20	-23	-26	-29	-32	-35	-38	-41	-44	-47	-50	-53	-56	-59
100	330	-15	-18	-21	-24	-27	-30	-33	-36	-39	-42	-45	-48	-51	-54	-57	-60
100	340	-16	-19	-22	-25	-28	-31	-34	-37	-40	-43	-46	-49	-52	-55	-58	-61
100	350	-17	-20	-23	-26	-29	-32	-35	-38	-41	-44	-47	-50	-53	-56	-59	-62
100	360	-18	-21	-24	-27	-30	-33	-36	-39	-42	-45	-48	-51	-54	-57	-60	-63
100	370	-19	-22	-25	-28	-31	-34	-37	-40	-43	-46	-49	-52	-55	-58	-61	-64
100	380	-20	-23	-26	-29	-32	-35	-38	-41	-44	-47	-50	-53	-56	-59	-62	-65
100	390	-21	-24	-27	-30	-33	-36	-39	-42	-45	-48	-51	-54	-57	-60	-63	-66
100	400	-22	-25	-28	-31	-34	-37	-40	-43	-46	-49	-52	-55	-58	-61	-64	-67
100	410	-23	-26	-29	-32	-35	-38	-41	-44	-47	-50	-53	-56	-59	-62	-65	-68
100	420	-24	-27	-30	-33	-36	-39	-42	-45	-48	-51	-54	-57	-60	-63	-66	-69
100	430	-25	-28	-31	-34	-37	-40	-43	-46	-49	-52	-55	-58	-61	-64	-67	-70
100	440	-26	-29	-32	-35	-38	-41	-44	-47	-50	-53	-56	-59	-62	-65	-68	-71
100	450	-27	-30	-33	-36	-39	-42	-45	-48	-51	-54	-57	-60	-63	-66	-69	-72
100	460	-28	-31	-34	-37	-40	-43	-46	-49	-52	-55	-58	-61	-64	-67	-70	-73
100	470	-29	-32	-35	-38	-41	-44	-47	-50	-53	-56	-59	-62	-65	-68	-71	-74
100	480	-30	-33	-36	-39	-42	-45	-48	-51	-54	-57	-60	-63	-66	-69	-72	-75
100	490	-31	-34	-37	-40	-43	-46	-49	-52	-55	-58	-61	-64	-67	-70	-73	-76
100	500	-32	-35	-38	-41	-44	-47	-50	-53	-56	-59	-62	-65	-68	-71	-74	-77
100	510	-33	-36	-39	-42	-45	-48	-51	-54	-57	-60	-63	-66	-69	-72	-75	-78
100	520	-34	-37	-40	-43	-46	-49	-52	-55	-58	-61	-64	-67	-70	-73	-76	-79
100	530	-35	-38	-41	-44	-47	-50	-53	-56	-59	-62	-65	-68	-71	-74	-77	-80
100	540	-36	-39	-42	-45	-48	-51	-54	-57	-60	-63	-66	-69	-72	-75	-78	-81
100	550	-37	-40	-43	-46	-49	-52	-55	-58	-61	-64	-67	-70	-73	-76	-79	-82
100	560	-38	-41	-44	-47	-50	-53	-56	-59	-62	-65	-68	-71	-74	-77	-80	-83
100	570	-39	-42	-45	-48	-51	-54	-57	-60	-63	-66	-69	-72	-75	-78	-81	-84
100	580	-40	-43	-46	-49	-52	-55	-58	-61	-64	-67	-70	-73	-76	-79	-82	-85
100	590	-41	-44	-47	-50	-53	-56	-59	-62	-65	-68	-71	-74	-77	-80	-83	-86
100	600	-42	-45	-48	-51	-54	-57	-60	-63	-66	-69	-72	-75	-78	-81	-84	-87
100	610	-43	-46	-49	-52	-55	-58	-61	-64	-67	-70	-73	-76	-79	-82	-85	-88
100	620	-44	-47	-50	-53	-56	-59	-62	-65	-68	-71	-74	-77	-80	-83	-86	-89
100	630	-45	-48	-51	-54	-57	-60	-63	-66	-69	-72	-75	-78	-81	-84	-87	-90
100	640	-46	-49	-52	-55	-58	-61	-64	-67	-70	-73	-76	-79	-82	-85	-88	-91
100	650	-47	-50	-53	-56	-59	-62	-65	-68	-71	-74	-77	-80	-83	-86	-89	-92
100	660	-48	-51	-54	-57	-60	-63	-66	-69	-72	-75	-78	-81	-84	-87	-90	-93
100	670	-49	-52	-55	-58	-61	-64	-67	-70	-73	-76	-79	-82	-85	-88	-91	-94
100	680	-50	-53	-56	-59	-62	-65	-68	-71	-74	-77	-80	-83	-86	-89	-92	-95
100	690	-51	-54	-57	-60	-63	-66	-69	-72	-75	-78	-81	-84	-87	-90	-93	-96
100	700	-52	-55	-58	-61	-64	-67	-70	-73	-76	-79	-82	-85	-88	-91	-94	-97
100	710	-53	-56	-59	-62	-65	-68	-71	-74	-77	-80	-83	-86	-89	-92	-95	-98
100	720	-54	-57	-60	-63	-66	-69	-72	-75	-78	-81	-84	-87	-90	-93	-96	-99
100	730	-55	-58	-61	-64	-67	-70	-73	-76	-79	-82	-85	-88	-91	-94	-97	-100
100	740	-56	-59	-62	-65	-68	-71	-74	-77	-80	-83	-86	-89	-92	-95	-98	-101
100	750	-57	-60	-63	-66	-69	-72	-75	-78	-81	-84	-87	-90	-93	-96	-99	-102
100	760	-58	-61	-64	-67	-70	-73	-76	-79	-82	-85	-88	-91	-94	-97	-100	-103
100	770	-59	-62	-65	-68	-71	-74	-77	-80	-83	-86	-89	-92	-95	-98	-101	-104
100	780	-60	-63	-66	-69	-72	-75	-78	-81	-84	-87	-90	-93	-96	-99	-102	-105
100	790	-61	-64	-67	-70	-73	-76	-79	-82	-85	-88	-91	-94	-97	-100	-103	-106
100	800	-62	-65	-68	-71	-74	-77	-80	-83	-86	-89	-92	-95	-98	-101	-104	-107
100	810	-63	-66	-69	-72	-75	-78	-81	-84	-87	-90	-93	-96	-99	-102	-105	-108
100	820	-64	-67	-70	-73	-76	-79	-82	-85	-88	-91	-94	-97	-100	-103	-106	-109
100	830	-65	-68	-71	-74	-77	-80	-83	-86	-89	-92	-95	-98	-101	-104	-107	-110
100	840	-66	-69	-72	-75	-78	-81	-84	-87	-90	-93	-96	-99	-102	-105	-108	-111
100	850	-67	-70	-73	-76	-79	-82	-85	-88	-91	-94	-97	-100	-103	-106	-109	-112
100	860	-68	-71	-74	-77	-80	-83	-86	-89	-92	-95	-98	-101	-104	-107	-110	-113
100	870	-69	-72	-75	-78	-81	-84	-87	-90	-93	-96	-99	-102	-105	-108	-111	-114
100	880	-70	-73	-76	-79	-82	-85	-88	-91	-94	-97	-100	-103	-106	-109	-112	-115
100	890	-71	-74	-77	-80	-83	-86	-89	-92	-95	-98	-101	-104	-107	-110	-113	-116
100	900	-72	-75	-78	-81	-84	-87	-90	-93	-96	-99	-102	-105	-108	-111	-114	-117
100	910	-73	-76	-79	-82	-85	-88	-91	-94	-97	-100	-103	-106	-109			

ORIGINAL PAGE IS
OF POOR QUALITY

Table 17: ΔZ (Dusk - Dawn)/2, units nT.

LATITUDE RANGE	LONGITUDE RANGE																					
	-30	-27	-24	-21	-18	-15	-12	-9	-6	-3	0	3	6	9	12	15	18	21	24	27	30	
174 TO 175	-1	2	1	3	7	10	10	9	7	5	-1	3	4	5	5	4	3	2	1	0	-1	-2
174 TO 174	-1	2	2	3	7	10	10	9	7	5	-1	3	4	5	5	4	3	2	1	0	-1	-2
174 TO 165	-1	2	3	4	5	5	5	5	5	5	-1	1	2	3	4	5	5	4	3	2	1	0
174 TO 160	-1	2	4	4	4	4	4	4	4	4	-1	1	2	3	4	5	5	4	3	2	1	0
174 TO 155	-1	2	4	4	4	4	4	4	4	4	-1	1	2	3	4	5	5	4	3	2	1	0
174 TO 150	-1	2	4	4	4	4	4	4	4	4	-1	1	2	3	4	5	5	4	3	2	1	0
174 TO 145	-1	2	4	4	4	4	4	4	4	4	-1	1	2	3	4	5	5	4	3	2	1	0
174 TO 140	-1	2	4	4	4	4	4	4	4	4	-1	1	2	3	4	5	5	4	3	2	1	0
174 TO 135	-1	2	4	4	4	4	4	4	4	4	-1	1	2	3	4	5	5	4	3	2	1	0
174 TO 130	-1	2	4	4	4	4	4	4	4	4	-1	1	2	3	4	5	5	4	3	2	1	0
174 TO 125	-1	2	4	4	4	4	4	4	4	4	-1	1	2	3	4	5	5	4	3	2	1	0
174 TO 120	-1	2	4	4	4	4	4	4	4	4	-1	1	2	3	4	5	5	4	3	2	1	0
174 TO 115	-1	2	4	4	4	4	4	4	4	4	-1	1	2	3	4	5	5	4	3	2	1	0
174 TO 110	-1	2	4	4	4	4	4	4	4	4	-1	1	2	3	4	5	5	4	3	2	1	0
174 TO 105	-1	2	4	4	4	4	4	4	4	4	-1	1	2	3	4	5	5	4	3	2	1	0
174 TO 100	-1	2	4	4	4	4	4	4	4	4	-1	1	2	3	4	5	5	4	3	2	1	0
174 TO 95	-1	2	4	4	4	4	4	4	4	4	-1	1	2	3	4	5	5	4	3	2	1	0
174 TO 90	-1	2	4	4	4	4	4	4	4	4	-1	1	2	3	4	5	5	4	3	2	1	0
174 TO 85	-1	2	4	4	4	4	4	4	4	4	-1	1	2	3	4	5	5	4	3	2	1	0
174 TO 80	-1	2	4	4	4	4	4	4	4	4	-1	1	2	3	4	5	5	4	3	2	1	0
174 TO 75	-1	2	4	4	4	4	4	4	4	4	-1	1	2	3	4	5	5	4	3	2	1	0
174 TO 70	-1	2	4	4	4	4	4	4	4	4	-1	1	2	3	4	5	5	4	3	2	1	0
174 TO 65	-1	2	4	4	4	4	4	4	4	4	-1	1	2	3	4	5	5	4	3	2	1	0
174 TO 60	-1	2	4	4	4	4	4	4	4	4	-1	1	2	3	4	5	5	4	3	2	1	0
174 TO 55	-1	2	4	4	4	4	4	4	4	4	-1	1	2	3	4	5	5	4	3	2	1	0
174 TO 50	-1	2	4	4	4	4	4	4	4	4	-1	1	2	3	4	5	5	4	3	2	1	0
174 TO 45	-1	2	4	4	4	4	4	4	4	4	-1	1	2	3	4	5	5	4	3	2	1	0
174 TO 40	-1	2	4	4	4	4	4	4	4	4	-1	1	2	3	4	5	5	4	3	2	1	0
174 TO 35	-1	2	4	4	4	4	4	4	4	4	-1	1	2	3	4	5	5	4	3	2	1	0
174 TO 30	-1	2	4	4	4	4	4	4	4	4	-1	1	2	3	4	5	5	4	3	2	1	0
174 TO 25	-1	2	4	4	4	4	4	4	4	4	-1	1	2	3	4	5	5	4	3	2	1	0
174 TO 20	-1	2	4	4	4	4	4	4	4	4	-1	1	2	3	4	5	5	4	3	2	1	0
174 TO 15	-1	2	4	4	4	4	4	4	4	4	-1	1	2	3	4	5	5	4	3	2	1	0
174 TO 10	-1	2	4	4	4	4	4	4	4	4	-1	1	2	3	4	5	5	4	3	2	1	0
174 TO 5	-1	2	4	4	4	4	4	4	4	4	-1	1	2	3	4	5	5	4	3	2	1	0
174 TO 0	-1	2	4	4	4	4	4	4	4	4	-1	1	2	3	4	5	5	4	3	2	1	0
174 TO -5	-1	2	4	4	4	4	4	4	4	4	-1	1	2	3	4	5	5	4	3	2	1	0
174 TO -10	-1	2	4	4	4	4	4	4	4	4	-1	1	2	3	4	5	5	4	3	2	1	0
174 TO -15	-1	2	4	4	4	4	4	4	4	4	-1	1	2	3	4	5	5	4	3	2	1	0
174 TO -20	-1	2	4	4	4	4	4	4	4	4	-1	1	2	3	4	5	5	4	3	2	1	0
174 TO -25	-1	2	4	4	4	4	4	4	4	4	-1	1	2	3	4	5	5	4	3	2	1	0
174 TO -30	-1	2	4	4	4	4	4	4	4	4	-1	1	2	3	4	5	5	4	3	2	1	0